

ELEMENTS OF FABRIC-REINFORCED
SOIL BEHAVIOR

By

ALY MAHMOUD FAWZY

Bachelor of Civil Engineering
Cairo University
Cair, Egypt
1974

Master of Science
Oklahoma State University
Stillwater, Oklahoma
1977

Submitted to the Faculty of the Graduate College
of the Oklahoma State University
in partial fulfillment of the requirements
for the Degree of
DOCTOR OF PHILOSOPHY
July, 1979

Thess
1979D
F2812
cop. 2

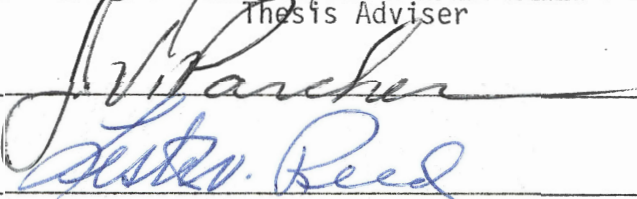


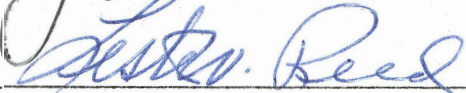
ELEMENTS OF FABRIC-REINFORCED
SOIL BEHAVIOR

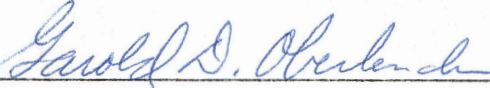
Thesis Approved:

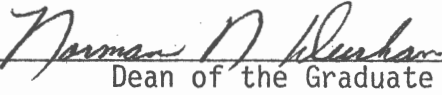


Thesis Adviser









Dean of the Graduate College

1041437

ACKNOWLEDGMENTS

The author would like to express his deep and sincere gratitude to Dr. T. A. Haliburton, major adviser, from whom he received generous encouragement and valuable help at all stages of this study. His critical comments and technical implications were extremely helpful in presenting the matter contained in this thesis.

Sincere appreciation is also expressed to Dr. James V. Parcher, committee chairman, Dr. W. P. Dawkins, Dr. G. Oberlender and Dr. L. Reed, committee members, for their invaluable guidance and inspiration throughout this study.

To
T. A. Haliburton
The Professor, The Friend

TABLE OF CONTENTS

Chapter	Page
I. INTRODUCTION	1
1.1 General	1
1.2 Scope	2
II. REVIEW AND DISCUSSION OF PREVIOUS WORK	3
2.1 Experimental Analysis	3
2.2 Design Aspects of Earth Dams Reinforced with Fabrics	10
III. MECHANICS OF REINFORCED EARTH	15
3.1 General	15
3.2 Development of Active Earth Pressure	15
3.3 Lateral Restraint	16
3.4 Finite Element Method	25
IV. METHOD OF ANALYSIS	29
4.1 General	29
4.2 Plate Equilibrium Equations	29
4.3 Discrete Element Model	35
4.4 Nonlinear Analysis	37
V. DESIGN PROCEDURE	39
5.1 General	39
5.2 Footing Design	39
5.3 Slope Stability	44
VI. UNCERTAINTY AND PROBABILISTIC DESIGN	52
6.1 General	52
6.2 Gaussian Distribution	53
6.3 Estimation	53
VII. CASE STUDY	60
7.1 Statement and Description of the Problem	60
7.2 Embankment-Foundation Data	60
7.3 Fabric Data	62
7.4 Location of Fabric in Embankment	65

Chapter	Page
7.5 Results of Analysis	65
7.6 Conclusions	67
VIII. SUMMARY AND RECOMMENDATIONS	69
REFERENCES	70
APPENDIX A - PROPERTIES OF MEMBRANE MODEL	72
APPENDIX B - DESIGN OF MINIMUM ANCHORAGE LENGTH	88
APPENDIX C - EXAMPLE PROBLEMS	93

LIST OF TABLES

Table	Page
I. Summary of Fabric Wrap Direction Laboratory Test Results	63
II. Type and Location of Fabric Reinforcement in Embankment	64
III. Assumptions Used in Analysis	65
IV. Results of Analysis	66

LIST OF FIGURES

Figure	Page
1. Load Test for a Reinforced Earth Mass	4
2. Pullout Test	9
3. Reinforced Earth Embankment	12
4. Slice Method in Reinforced Embankments	13
5. Stress Change in a Laterally Expanding Soil Mass	17
6. Stress Change in a Standard Triaxial Test	18
7. Failure Conditions for Constant σ_r	19
8. Constant σ_r Related to Strength of Reinforcement	21
9. Failure Conditions for $\sigma_r = \sigma_1 C$	22
10. Variable σ_r Related to Vertical Stress	24
11. Combined Cohesion and Friction Effects	26
12. Membrane Forces on Plate Element	30
13. Membrane Forces on Deformed Plate Element	32
14. Strain, ϵ_x , Due to Large Deflections	34
15. Membrane Model	36
16. Factors Affecting Fabric Usefulness	41
17. Reinforced Footing Foundation	42
18. Deformed Fabric Under Footing Load	43
19. Free Body Diagram for Deformed Fabric	45
20. Pullout Test Apparatus	47
21. Deformed Fabric in Slope Stability Problem	48
22. Free Body Diagram for the Sliced Mass	49

Figure	Page
23. Gaussian Distribution Curve	54
24. General Location of Embankment Test Section in Mobile Harbor, Alabama	61
25. Simplified Fabric-Reinforced Embankment Section Used for Analysis Purposes	68
26. Plane Stress Element	75
27. Member of Discrete-Element Model	76
28. Shearing Deformation of Discrete Element	80
29. Deformation of an Elastic Bar of the Discrete Element	81
30. Plate Element With In-Plane Loads	83
31. Discrete Element Representation of Plate Element	85
32. Forces in Elastic Bars of Membrane Element	87
33. Rheological Model	90
34. Deformed Fabric	95
35. Reinforced Embankment	98

LIST OF SYMBOLS

a	dimension of footing
A	dimension of fabric reinforcement
A_s	cross-sectional area of reinforcement
B	horizontal dimension of soil mass affected by fabric inclusion
C	constant relating prestress σ_r to major stress σ_1
C_r	apparent cohesion as a result of reinforcement
d	depth of reinforcement
E	modulus of elasticity
f	averaging factor to account for the effect of uneven distribution of the shear stress
h_x, h_y	discrete element length
H	vertical dimension of soil mass affected by fabric inclusion
K	subgrade coefficient
K_a	coefficient of active earth pressure
K_{ar}	coefficient of active earth pressure of reinforced soil
K_0	coefficient of earth pressure at rest
l_r	minimum anchorage length
M_D	driving moment
M_{sf}	stabilizing moment as a result of fabric inclusion
N_x, N_y, N_{xy}	in-plane force
P	column load
t	membrane thickness

T_F	force compatible with the design displacement
T_L	pullout force measured in the pullout test
u	displacement in X direction
u_0	displacement of the strip tested in laboratory
u'_0	strain of the strip tested in laboratory
v	displacement in Y direction
w	displacement in Z direction
$\sigma_x, \sigma_y, \sigma_{xy}$	normal and shearing stresses in membrane model
σ_r	prestress due to reinforcement
σ_1	major normal stress
σ_{1u}	major normal stress in unreinforced mass
σ_{3u}	minor normal stress in unreinforced mass
σ^2	variance of the population
$\epsilon_x, \epsilon_y, \gamma_{xy}$	strains in membrane model
ϕ_r	angle of internal friction for reinforced soil
Ω	parameter space

CHAPTER I

INTRODUCTION

1.1 General

During the last decade reinforcing soil with tension-resistant material has been widely implemented into practice. Generally it is used for strengthening a soil foundation, and most experimental and theoretical studies have been devoted to evaluating the strength of reinforced soil-filled foundations. Model tests (16) have shown that reinforcement increases both strength and rigidity of a soil foundation. Now, metal is generally used for the reinforcement but the writer believes that synthetic materials will soon be widely applied for this purpose. Reinforcement made of films of different, non-woven material, possesses such favorable qualities as low cost, chemical stability, light weight, easy transportability (for example, in rolls), easy joining (by means of heat or glue), high mechanical strength, etc. Chemical stability of these materials permits the manufacture of very thin sheets that provide for much larger surface areas without increasing the weight. This is important because larger surface area means larger contact area with soil that in turn contributes to better soil-reinforcement performance.

Recently, synthetic reinforcement has been widely implemented into construction on soft saturated soils especially for road construction

(14) (17) where non-woven synthetic type materials have been used. Application of such reinforcement also provides for better subgrade drainage.

1.2 Scope

The goals of this study are:

1. To explore the mechanics of reinforced earthwork.
2. To develop a mathematical model.
3. To suggest a design procedure.
4. To develop a statistical model.

CHAPTER II

REVIEW AND DISCUSSION OF PREVIOUS WORK

2.1 Experimental Analysis

2.1.1 General

Because the behavioral mechanism of the soil/fabric system is not yet well understood, extensive experimental work has been performed during the last decade to explore the system interaction.

These experiments can be divided into two main groups as follows:

1. Tests performed in the field.
2. Model-type tests.

2.1.2 Tests Performed in the Field

An investigation (14) was made concerning the influence of the inclusion of nonwoven synthetic fabric between a "soft" silty soil and an overlying gravel layer with respect to compactibility and bearing capacity. Figure 1 is a diagrammatic representation of the test.

Investigation of the deflection and the modulus of elasticity in both loading and unloading (E_{v1} , E_{v2}) during a plate load test included tests of both reinforced and unreinforced systems. Variables included the thickness of the gravel layer and the water content of the soft silt.

The conclusions can be summarized as follows:

1. The benefits of fabric inclusion can be expressed by an

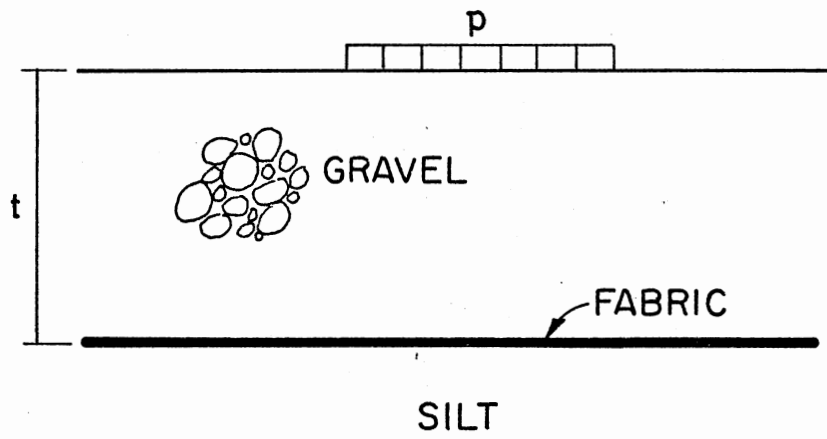


Figure 1. Load Test for a Reinforced Earth Mass

"improvement factor":

$$\text{Improvement factor} = \frac{\text{Modulus of elasticity after inclusion}}{\text{Modulus of elasticity before inclusion}}$$

It was found that fabric inclusion is more beneficial if the subgrade is softer.

2. Within certain limits, it is more beneficial to include fabric than to increase the subbase thickness (gravel layer).

2.1.3 Model-Type Tests

The stress-strain behavior of a unit cell of sand, when tested under plane strain conditions with and without a fabric membrane inclusion, has been investigated by McGown and Andrawes (16) at the University of Strathclyde in Glasgow.

The variable parameters were:

1. Placement void ratio.
2. Existence of fabric.
3. Fabric maximum strength.
4. Fabric orientation.

It was found that when the nonwoven fabrics were placed along the major principal plane (horizontal) they generally increased the strength of the system—although when the sands were placed at their minimum void ratio, a slight weakening was observed. The peak strength of the fabrics appeared to have some influence, but system strengthening was not directly proportional to it. More important than the strengthening was the fact that the strains to the peak strength were increased and the post-peak brittleness of the system was markedly reduced.

Such behavior, in fact, is in stark contrast to the influences of

metals and fabrics of low extensibility which inhibit strains. Thus, the fabric-included systems tested in this particular research are considered to have particular characteristics and have therefore been termed "ply-soil" systems to indicate their capability of accepting deformations, without disruption, above those which the soil media alone could accept. It was also found that when the fabrics were inclined to the major principal plane, i.e., to the horizontal, a definite anisotropic pattern of behavior could be established. At certain inclinations, essentially where the fabrics were inclined at an angle close to that of the shear failure plane, weakening of the system at all void ratios of sand was observed. This was a result of the soil/fabric friction being a little less than soil-soil friction and highlights the importance of surface properties of the inclusions.

2.1.4 Footing Model

The apparatus consists of a very strong narrow box; the front and back are composed of thick glass platens to permit photography.

Three groups of tests were conducted in this apparatus. The first group was with a single inclusion at various depths within a single layer of dense or loose sand. The second group was with two separate inclusions of fabric within either a layer of dense or loose sand. The third group involved inclusions of fabric placed at the interface of dense sand over either loose sand or rubber with the depth of dense sand varied between tests. The following parameters have been used:

1. Depth ratio = $\frac{\text{Depth of inclusion}}{\text{Width of footing}}$
2. Spacing ratio = $\frac{\text{Spacing of inclusions}}{\text{Width of footing}}$

3. Settlement ratio = $\frac{\text{Settlement of footing}}{\text{Width of footing}}$
4. Improvement factor (at any settlement ratio)
- $$= \frac{\text{Vertical footing stress with inclusions}}{\text{Vertical footing stress without inclusions}}$$

The model footing tests on dense or loose sand in general confirmed the findings of the unit cell tests previously stated, particularly when the load-deformation behavior of the footing was considered in association with interface deformation patterns observed through the glass sides of the model. In almost all cases, as with the unit cell, the inclusion of fabric increased the strength of the system. Indeed, the most critical factor tested appeared to be the positioning of the fabric membrane in the system, the depth ratio. When the internal major principal strain directions within the sand without inclusions are considered, it is evident that the best performance of fabric-included systems occurs when the fabric membrane lies across those strain directions and the least improvement or weakening occurs when the fabric lies along them. Thus the depth ratio is comparable in its effect, to the fabric inclination in the unit cell.

In those tests where dense sand overlaid loose sand or rubber, the critical influence of the depth ratio was borne out. In addition, the differences in improvement factors due to the inclusions at the interface of the dense sand with the loose sand and the rubber subsoils were shown to be in keeping with the relative improvements due to the dense sand overlays alone.

The deformation mechanisms without fabric were different; therefore, the influences of fabric inclusion were different. The very low friction or adhesion at the fabric rubber interface was also thought to

be an improvement factor in these tests. Finally, double fabric inclusions showed that the deformation modifications induced by an individual layer might interact with those induced by another individual layer to produce a greatly enhanced overall improvement, but as might be expected there was a critical positioning for the two layers in the system. Considerations of this positioning lead to the same conclusions as before with respect to the relative orientation of the inclusion with respect to the internal principal strains. Hence, the inclusion of highly extensible nonwoven fabrics in various essentially granular soil systems has been shown to somewhat strengthen but more particularly alter the deformation behavior of the systems and possibly make them subject to less disruption at higher strains. Thus, the use of extensible nonwoven fabrics would appear to be most advantageous in soil systems such as roads or embankments on very soft clays or peats which can accept or will inevitably be subject to large strains.

2.1.5 Pull-Out Tests

Pull-out tests have been performed by Schwab (20) and others using the model shown in Figure 2. In each test the pull-out force, normal and shear stresses, and displacement vectors have been measured. It has been found that:

1. The friction angle between the fabric and the sand is 10 percent lower than the angle of internal friction as determined by direct shear tests.
2. The friction angle between sand and fabric calculated from the results of the pull-out tests depends to a large extent on the deformation of the fabric, the relative density of the sand, and the surcharge. The calculated friction angle varied between wide limits.

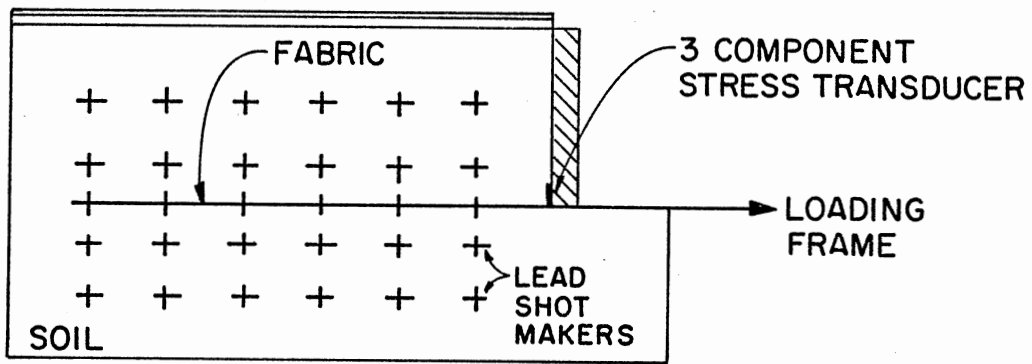


Figure 2. Pullout Test

3. The deformation at which the maximum frictional resistance was mobilized depends on the relative density of the sand and on the vertical pressure. The peak values for loose sand were larger than those for dense sand.

4. The pull-out tests indicate that the entire mass of sand above included fabric is affected by the reinforcement during the pull-out test. Below the fabric the zone of influence depends on the relative density and on the value of vertical pressure.

5. The shear and normal stress as against the wall increase with increasing pull force. At the start of a test the normal stress against the wall corresponded to the earth pressure at rest. The direction of the shear stress, initially downward, changed into an upward direction during loading, except when the vertical pressure was large.

2.2 Design Aspects of Earth Dams Reinforced with Fabrics

Recently, a few papers have been written about design aspects of earth dams reinforced with fabrics, and these papers analyze the design problem in a conventional way.

Christie and Echadi (7) suggested four possible modes of failure:

1. Sliding of base.
2. Failure of reinforcement in tension.
3. Shear failure through the reinforced embankment.
4. Failure of reinforcement through inadequate bond length. The first mode failure has nothing to do with the dam being reinforced. The other three failure modes are discussed hereafter.

2.2.1 Failure of Reinforcement in Tension

It is assumed that the reinforcement has to withstand a horizontal force created by active earth pressure. Thus, as shown in Fig. 3:

$$T \text{ (in fabric)} = \Delta H \cdot K_A \gamma Z \cos^2 \beta$$

where

K_A is the coefficient of active earth pressure.

Z is the vertical distance from the embankment crest.

β is the side slope angle.

ΔH is the vertical distance between fabrics.

The tension T should not exceed the maximum tensile strength of the fabric T_1 .

It is evident that the horizontal force has been underestimated because of considering active earth pressure with the smallest horizontal pressure that a mass of soil can mobilize. However, they said that this may be countered by the overestimate in the assumption of an infinite slope.

2.2.2 Shear Failure of Reinforced Embankment

The conventional slip circle analysis (slice method) was used, modified to take account of the tension provided by the reinforcement.

It should be mentioned here that it is doubtful to consider full tension in the fabric sheet for both splitting and shear failure modes, that is because there is a possibility of a "coupled" failure mode.

2.2.3 Bond failure of Reinforcement

It has been mentioned that failure of reinforcement through

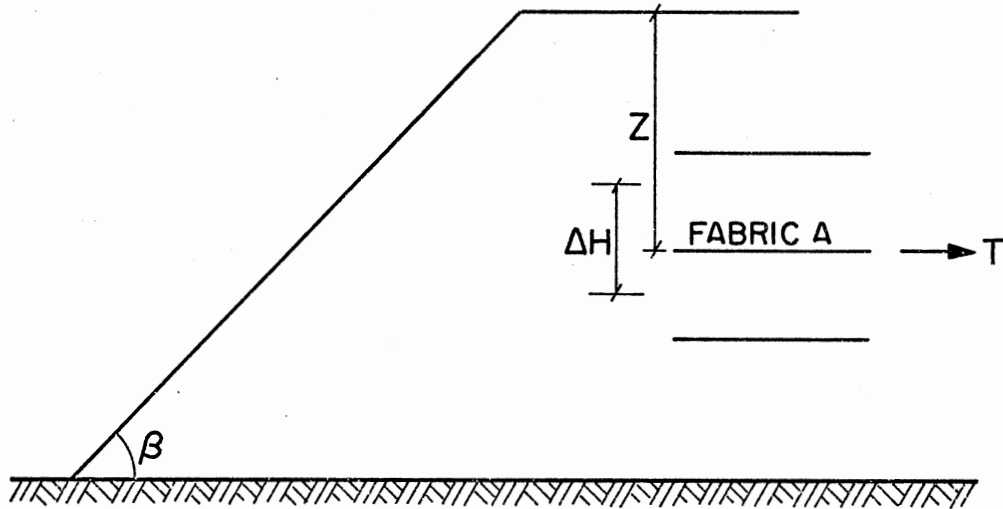


Figure 3. Reinforced Earth Embankment

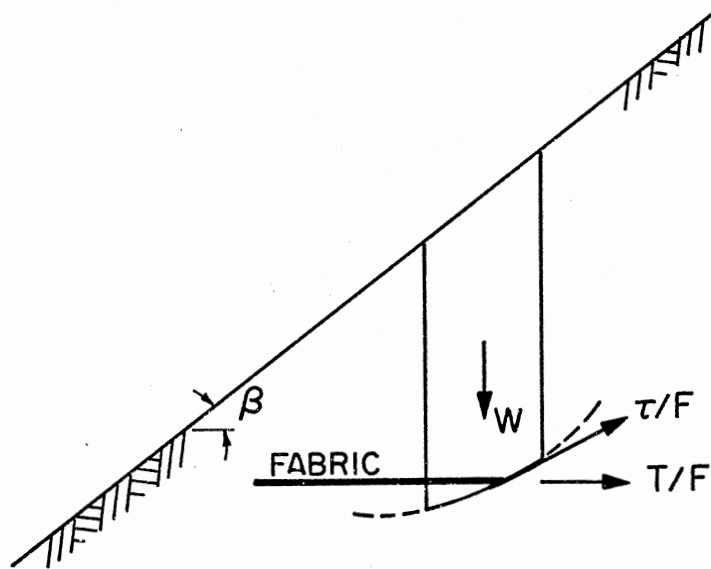


Figure 4. Slice Method in Reinforced Embankments

inadequate bond length should be checked at various points around the critical slip circle.

Two expressions for driving and resisting forces has been given.

$$\text{Driving force} = K_A \gamma Z \cos^2 \beta (\Delta H)$$

$$\text{Resisting force} = 2L\gamma Z \tan \psi$$

where

L = extension distance of the fabric sheet from the point considered;

ψ = angle of friction between the earth embankment soil and reinforcement.

CHAPTER III

MECHANICS OF REINFORCED EARTH

3.1 General

A reinforced earth mass might fail either by rupture of the reinforcement or by slippage between the reinforcement and the soil. Reinforcement of an earth mass can be seen as producing an intrinsic prestress, or lateral restraint, when failure conditions are approached. If the lateral prestress has a constant value related to the strength of the reinforcement, a cohesion intercept results. If it is proportional to the initial vertical stress, an increase in the angle of friction results.

3.2 Development of Active Earth Pressure

For geostatic stress conditions (referring to a homogeneous soil mass of large extent and horizontal surface) the horizontal stress σ_{3u} is usually expressed as

$$\sigma_{3u} = K_0 \sigma_{1u} \quad (3.1)$$

where K_0 is the coefficient of lateral stress at rest. Values normally range from 0.3 to 0.7; higher values are typical of overconsolidated soils. If a soil is allowed to expand horizontally, the lateral stress reduces to a minimum value, σ_a , the active earth pressure. The soil mass is then in a state of failure, also referred to as a Rankine state

of plastic equilibrium. The Mohr circle defining this condition touches the Mohr envelope, defined by the Mohr-Coulomb failure law as

$$\tau = C + \sigma \tan \phi \quad (3.2)$$

The same state of plastic equilibrium could be reached in a standard triaxial test, where σ_1 is increased while σ_3 remains constant. This is shown in Figure 6.

For simplicity and because in practical applications reinforcement is mainly used in sandy soils, the effect on soil strength is analyzed for the case of a cohesionless soil only.

3.3 Lateral Restraint

3.3.1 Constant Prestress σ_r

This case corresponds to conditions when failure of a reinforced soil mass occurs by rupture of the reinforcement. Lateral expansion of the soil mass creates prestress statically equivalent to a frictional force developed between the soil and the reinforcement with a maximum value determined by the tensile strength of the reinforcing material. For a constant prestress, σ_r , the increased strength is exhibited by adding "cohesion" C_r to the soil, as shown in Figure 7. An expression for C_r may be derived as follows:

$$\begin{aligned} \sigma_{1u} &= \frac{1}{K_a} \sigma_{3u} \\ &= \frac{1}{K_a} (\sigma_3 + \sigma_r) \\ &= \frac{1}{K_a} \sigma_3 + \frac{1}{K_a} \sigma_r \end{aligned}$$

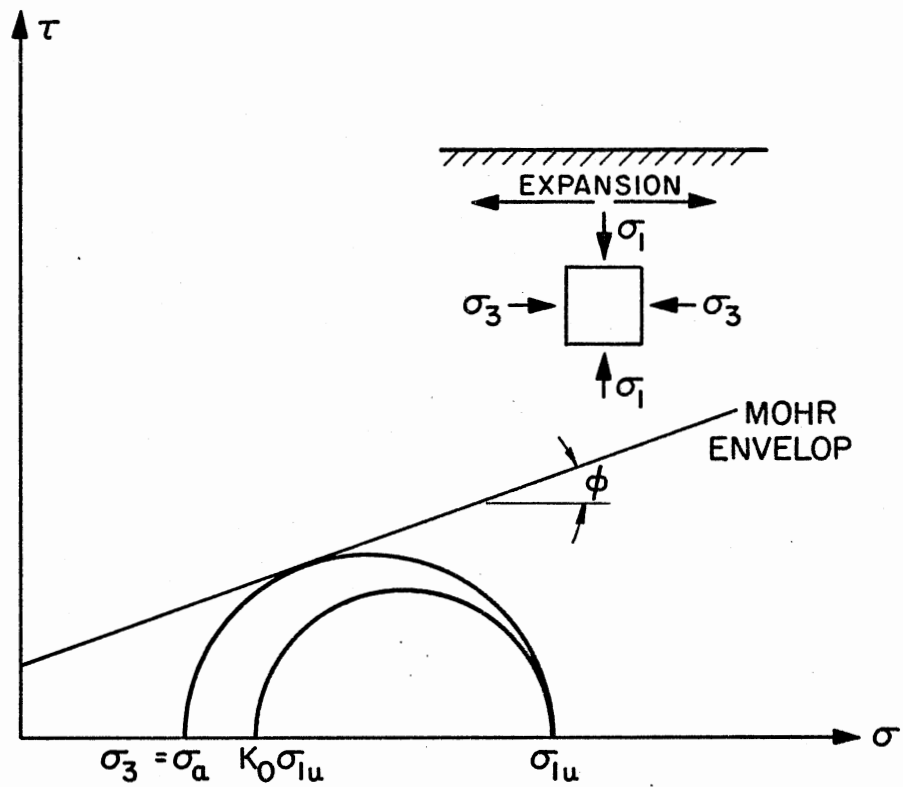


Figure 5. Stress Change in a Laterally Expanding Soil Mass

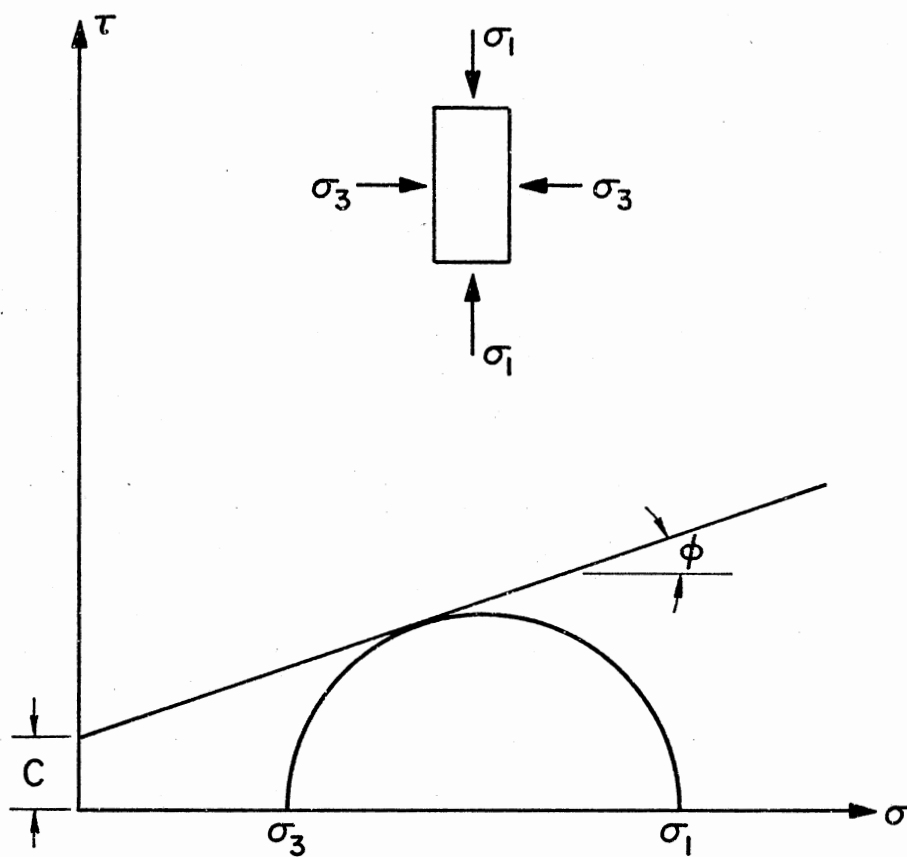


Figure 6. Stress Change in a Standard Triaxial Test

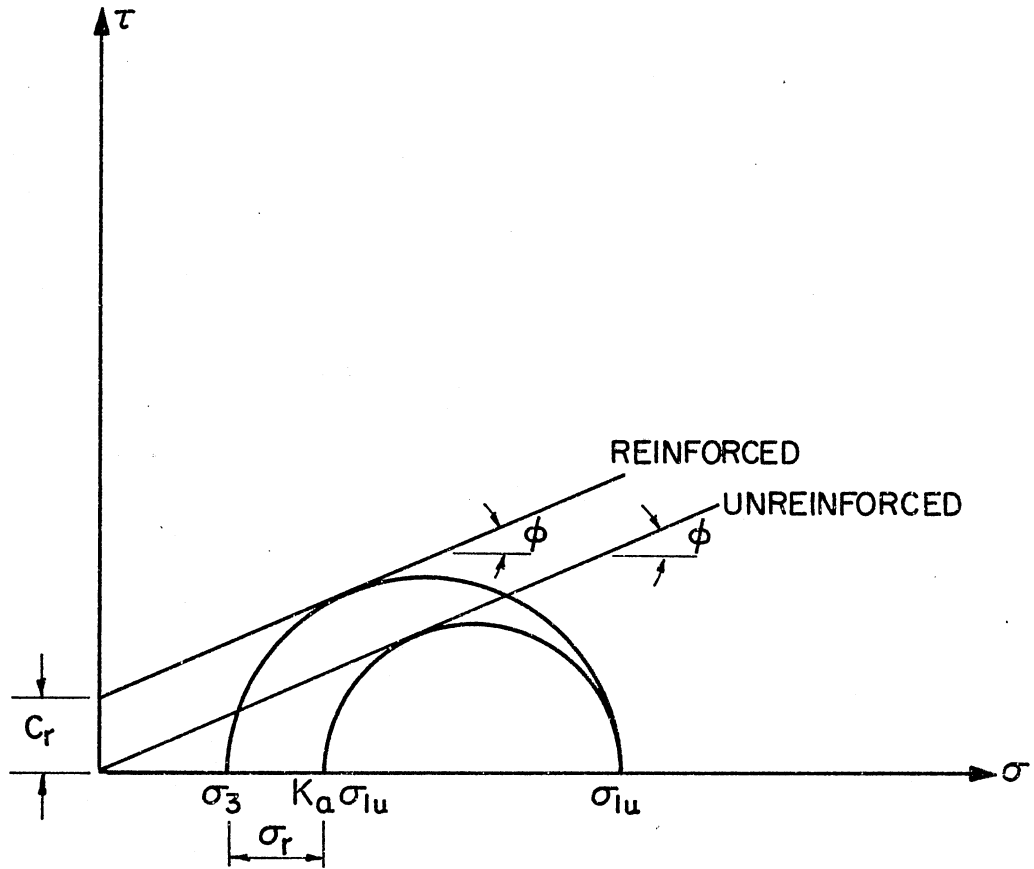


Figure 7. Failure Conditions for Constant σ_r

But

$$\sigma_1 = \frac{\sigma_3}{K_a} + \frac{2C_r}{\sqrt{K_a}}$$

Now, since $\sigma_1 = \sigma_{1u}$,

$$C_r = \frac{\sigma_r}{2\sqrt{K_a}} \quad (3.3)$$

For one-dimensional expansion over a horizontal interval B , with a vertical spacing H of reinforcement having a cross sectional area A_s and strength σ_s , as shown in Figure 8, the prestress is

$$\sigma_r = \sigma_s \frac{A_s}{BH} \quad (3.4)$$

3.3.2 Prestress σ_r Proportional to Vertical Stress σ_1

This case corresponds to conditions where the failure of the reinforced soil mass occurs by slippage between the reinforcement and the soil. Friction along horizontal reinforcement is directly proportional to the vertical stress

$$\sigma_r = C \sigma_1$$

This has the effect of increasing the friction angle, as shown in Figure 9. From Figure 9 we can write

$$\sigma_3 + \sigma_r = K_a \sigma_1$$

$$\frac{\sigma_3}{\sigma_1} + C = K_a$$

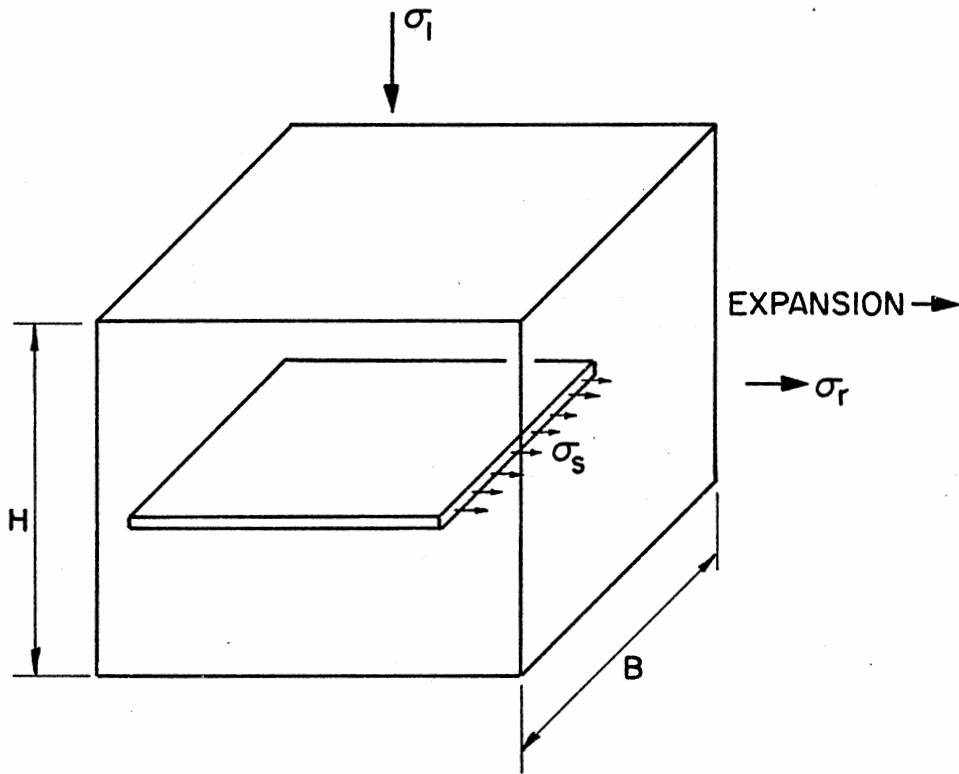


Figure 8. Constant σ_r Related to Strength of Reinforcement

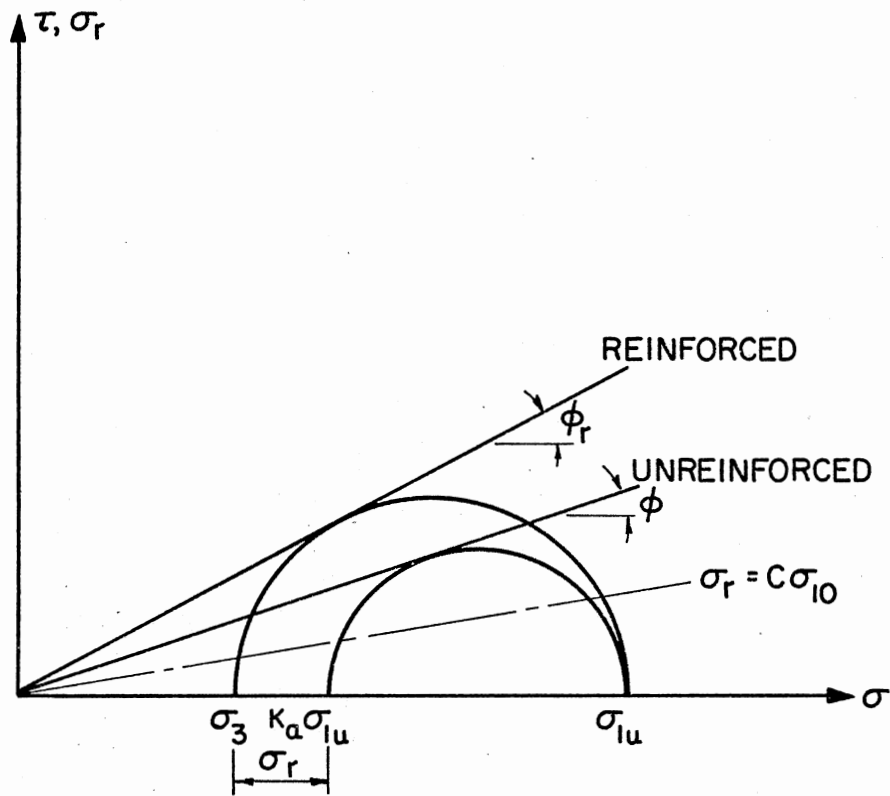


Figure 9. Failure Conditions for $\sigma_r = \sigma_l C$

since

$$\frac{\sigma_r}{\sigma_1} = c$$

But

$$\frac{\sigma_3}{\sigma_1} = K_{ar}$$

the coefficient of active pressure of the reinforced soil

$$K_{ar} + c = K_a$$

$$K_{ar} = K_a - c$$

$$\frac{1 - \sin\phi_r}{1 + \sin\phi_r} = K_a - c \quad (3.5)$$

where ϕ_r is the angle of internal friction of the reinforced soil mass.

Figure 10 illustrates how resistance to lateral expansion (= prestress) is developed by friction τ_s on the surface of the reinforcing material. The magnitude of τ_s will depend on the skin friction angle, δ , between the soil and reinforcement. It can be expected that τ_s is zero at midpoint and at the ends of the strip, and reaches maximum value equivalent to $\sigma_1 \tan\delta$ in between. Considering equilibrium (Figure 10)

$$\sigma_r BH = 2(\tau_{smax} f) B \frac{L}{2}$$

where f is an averaging factor to account for the effect of the uneven distribution of τ_s

$$\sigma_r = \sigma_1 \tan\delta \frac{B \cdot L}{BH} f$$

or

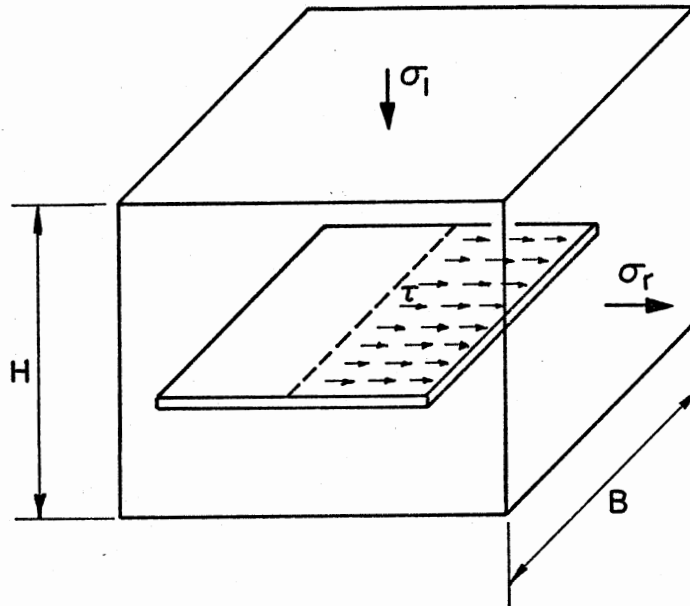


Figure 10. Variable σ_r Related to Vertical Stress

$$C = \tan \delta \frac{B^L}{BH} f \quad (3.6)$$

3.3.3 Combined Cohesion and Friction

Angle Effect

It is apparent that at low stress, failure in the reinforced soil mass tends to occur by slippage and at higher vertical stresses by rupture of the reinforcement. This is illustrated by Figure 11. Circle (a) describes the failure state for slippage, and circle (b) describes that for rupture of reinforcement. Prestress σ_r is assumed to increase proportionally to σ_1 up to a maximum value σ_{rmax} ; thereafter it remains constant.

3.4 Finite Element Method

In order to estimate the dimensions of the soil mass affected by fabric inclusion, the soil-fabric media needs to be solved. One of the most powerful methods that may be used to analyze the mechanism of soils with fabric inclusion is the finite element method. The use of the finite element method in conjunction with a high-speed digital computer provides an effective means for obtaining a reliable solution. However, the finite element model must be chosen carefully to satisfy material properties and boundary conditions. For example, most soils are considered to be incapable of resisting tension for sustained periods. It is therefore important to modify the finite element model in such a manner that no tensile stresses occur except in the fabric membrane. While the finite element method will not be used in the analytical procedure to be later recommended, it is useful to examine, briefly, some aspects of its application to this problem.

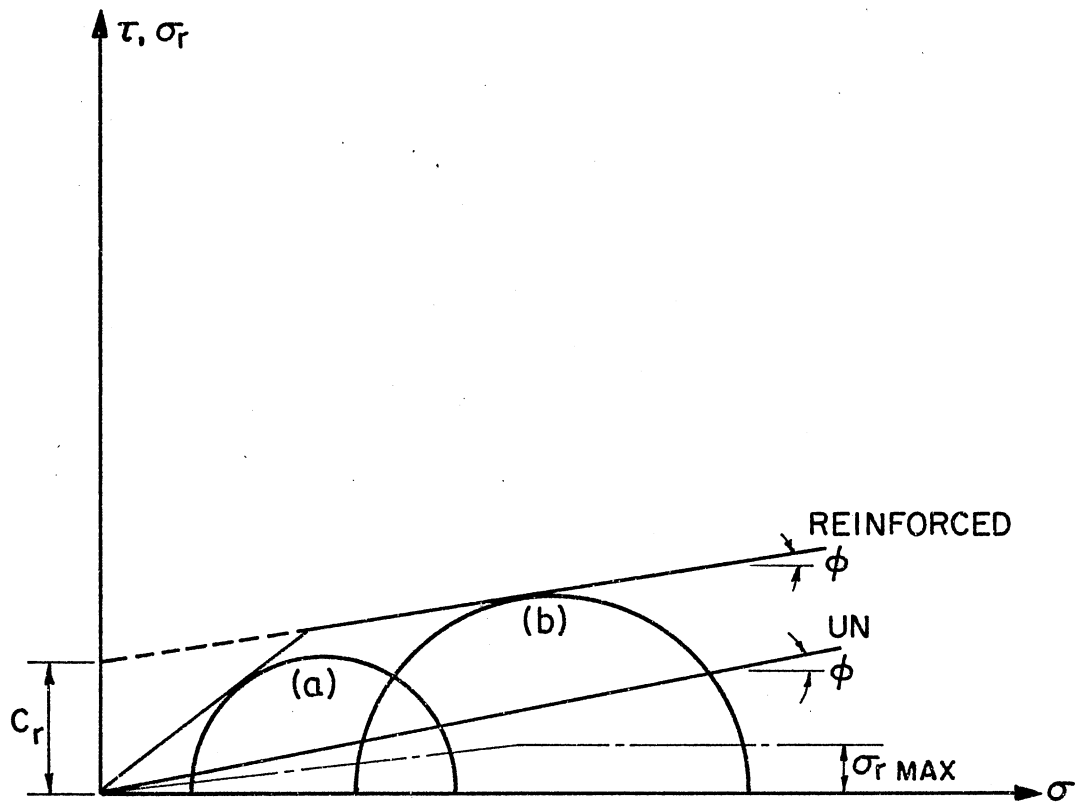


Figure 11. Combined Cohesion and Friction Effects

3.4.1 Nonlinearity

Since the deformations are large, the small deformation assumptions are not valid. For small deformations the displacement-strain relation is given by

$$\begin{aligned}\epsilon_x &= \frac{\partial u}{\partial x} \\ \epsilon_y &= \frac{\partial v}{\partial y} \\ \gamma_{xy} &= \frac{\partial v}{\partial x} + \frac{\partial u}{\partial y}\end{aligned}\tag{3.7}$$

For large deformation problems a nonlinear term should be included in Equation (3.7).

3.4.2 Compatibility

It is known that the assembly of the stiffness matrices of the element into one global stiffness matrix implies that compatibility among adjacent elements is satisfied. However, it is also known that the transmission of shearing stresses from cohesionless soil elements to the fabric membrane, which causes tension in the fabric, occurs only after a relative "slip" deformation between the soil and the fabric. This indicates that there is a relative movement between nodes which violates the compatibility principle. Hence, special elements which allow relative movement at the interface nodes should be used.

3.4.3 Simulating the "No Tension" Condition

As mentioned previously, a special provision should be taken to simulate the actual inability of the soil to transmit tension. Bell (4) tried to simulate the no-tension condition by:

1. Assuming the embankment is a linear orthotropic elastic material with Poisson's ratio equal to zero; and
2. Assuming that the elastic modulus in a horizontal direction is very small compared to the elastic modulus in a vertical direction.

The author disagrees with the above assumptions for simulating the no-tension property. The drastic reduction of the elastic modulus in the horizontal direction implies that the material is very "soft" in the horizontal direction, i.e., not capable of transmitting either tension or compression, which is not true. The assumption that Poisson's ratio is zero is also incorrect, because a given vertical stress or strain must induce stress or strain in the horizontal direction.

Without these assumptions, iterative methods must be used to obtain a solution. Two such procedures are:

Method 1:

1. Solve the problem without any provisions.
2. Assign zero modulus of elasticity at the particular elements that have tensile stresses from step 1, and solve the problem again.
3. Repeat step 2 until a stable solution is obtained.

Method 2:

1. Apply a small portion (5 to 10%) of the applied loads.
2. Assign zero modulus of elasticity to those elements where tension exists before the next portion of the load is applied.

CHAPTER IV

METHOD OF ANALYSIS

4.1 General

For small deflection ($w < 0.2t$) classic plate theory gives sufficiently accurate results. When the magnitude of the deflections increases beyond a certain level ($w < 0.3t$), large deflection theory must be used.

Although the large deflection theory of plates assumes that the deflections are equal to or larger than the plate thickness, the deflection should remain small relative to the other dimensions of the plate.

The strain in the middle surface must be considered for the large deflection analysis of thin plates. These supplementary strains (membrane strains) are expressed by nonlinear equations, and the solution of these equations is available for only a limited class of problems. Because of the curvature of the deformed middle surface of the plate, the supplementary tensile stresses, which resist the applied vertical loads, are completely transmitted by membrane action of the plate.

4.2 Plate Equilibrium Equations

From a plate element shown in Figure 12, equilibrium equations of forces in the X-Y plane are

$$\frac{\partial N_x}{\partial x} + \frac{\partial N_{yx}}{\partial y} = 0 \quad (4.1)$$

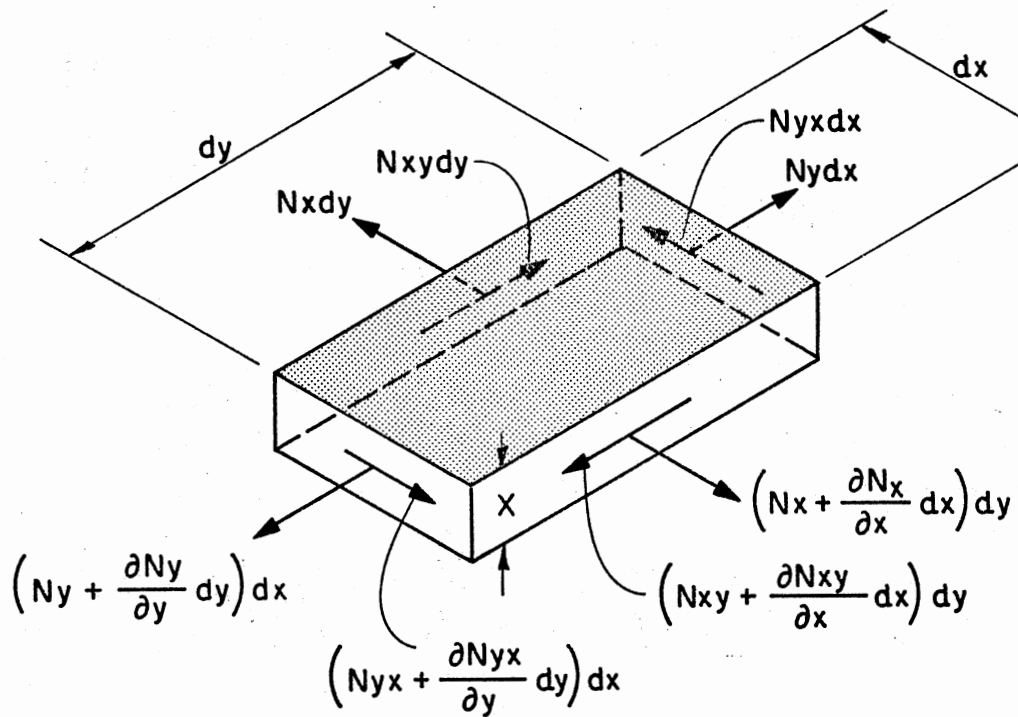


Figure 12. Membrane Forces on Plate Element

$$\frac{\partial N_{xy}}{\partial x} + \frac{\partial N_y}{\partial y} = 0 \quad (4.2)$$

In considering the equilibrium of the $dx dy$ element in the direction of the Z axis, for the sake of simplicity it is assumed that the far sides of the plate element are fixed and lie in the X - Y plane (see Figure 13). The projection of the membrane forces on the Z axis gives

$$\begin{aligned} & (N_x + \frac{\partial N_x}{\partial x} dx) dy \frac{\partial^2 w}{\partial x^2} dx + (N_y + \frac{\partial N_y}{\partial y} dy) dx \frac{\partial^2 w}{\partial y^2} dy \\ & + (N_{xy} + \frac{\partial N_{xy}}{\partial x} dx) dy \frac{\partial^2 w}{\partial x \partial y} dx + (N_{yx} + \frac{\partial N_{yx}}{\partial y} dy) dx \frac{\partial^2 w}{\partial x \partial y} dy \\ & = P_z(x,y) + kw(x,y) \end{aligned} \quad (4.3)$$

which, after neglecting small quantities of a higher order, becomes

$$N_x \frac{\partial^2 w}{\partial x^2} + N_y \frac{\partial^2 w}{\partial y^2} + 2N_{xy} \frac{\partial^2 w}{\partial x \partial y} = P_z(x,y) + k_w(x,y) \quad (4.4)$$

where k is the subgrade reaction coefficient.

Equation (4.4) is applicable in both small and large deflections.

If the Airy stress function ϕ is defined so that

$$\begin{aligned} N_x &= t \frac{\partial^2 \phi}{\partial y^2} \\ N_y &= t \frac{\partial^2 \phi}{\partial x^2} \\ N_{xy} &= N_{yx} = -t \frac{\partial^2 \phi}{\partial x \partial y} \end{aligned} \quad (4.5)$$

then it is clear that Equation (4.4) contains two unknowns (w, ϕ). Hence an additional equation, which relates the deflections and the stress function, is required. This is obtained in the form of a compatibility

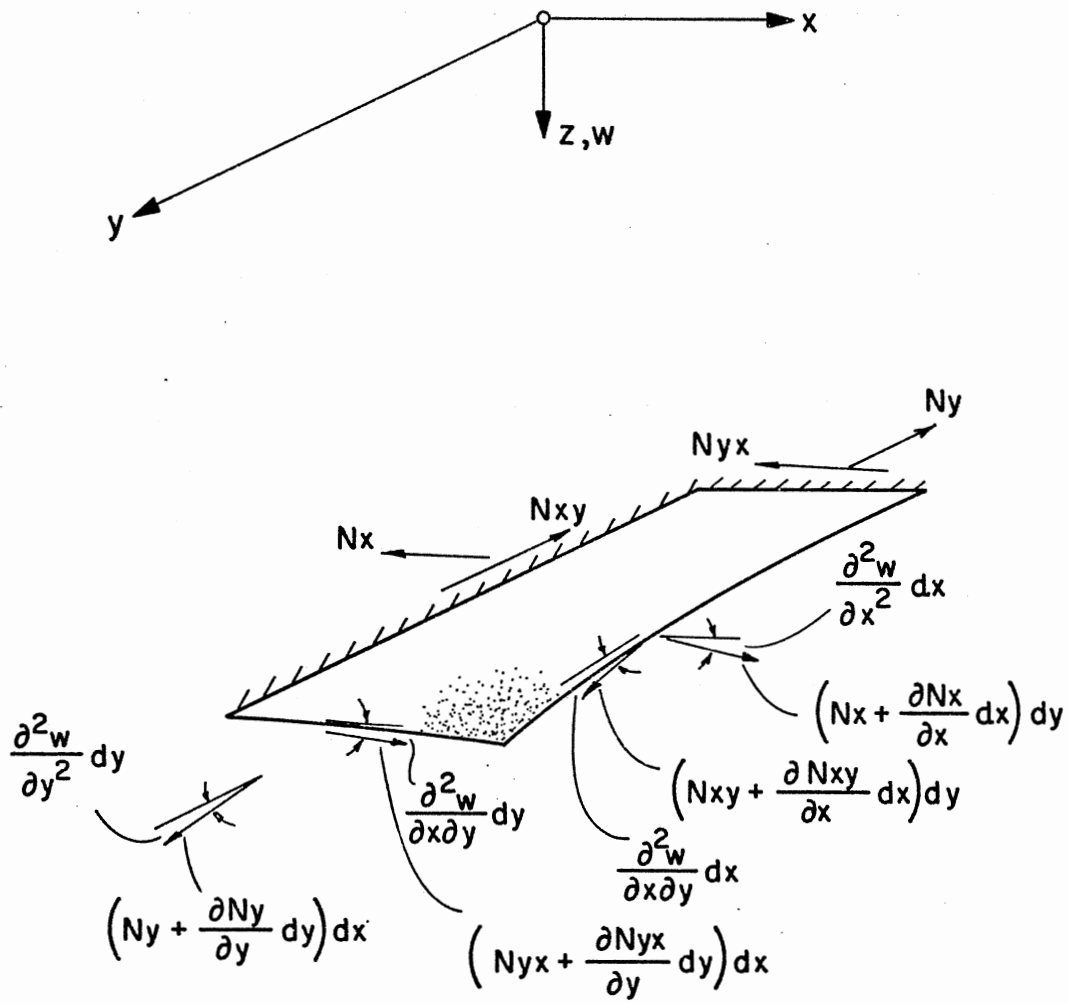


Figure 13. Membrane Forces on Deformed Plate Element

equation, in which the nonlinear terms in the large deflection strain-displacement expression (Figure 14) are also considered.

$$\epsilon_x = \frac{\partial u}{\partial x} + \frac{1}{2} \left(\frac{\partial w}{\partial x} \right)^2 = \frac{1}{Et} (N_x - N_y) \quad (4.6a)$$

$$\epsilon_y = \frac{\partial v}{\partial y} + \frac{1}{2} \left(\frac{\partial w}{\partial y} \right)^2 = \frac{1}{Et} (N_y - N_x) \quad (4.6b)$$

$$\gamma_{xy} = \frac{\partial u}{\partial y} + \frac{\partial v}{\partial x} + \frac{\partial w}{\partial x} \frac{\partial w}{\partial y} = \frac{2(1+\mu) N_{xy}}{Et} \quad (4.6c)$$

If we eliminate, by successive differentiation, the displacement components and replace membrane forces using Equation (4.5), then the pertinent compatibility equation is

$$\nabla^4 \phi = E \left[\left(\frac{\partial^2 w}{\partial x^2} \right)^2 - \frac{\partial^2 w}{\partial x^2} \frac{\partial^2 w}{\partial y^2} \right] \quad (4.7)$$

Using Equations (4.4) and (4.6), the governing differential equations of the large deflection theory can be written in a more condensed form:

$$t \left[\frac{\partial^2 w}{\partial x^2} \frac{\partial^2 \phi}{\partial y^2} + \frac{\partial^2 w}{\partial y^2} \frac{\partial^2 \phi}{\partial x^2} - 2 \frac{\partial^2 w}{\partial x \partial y} \frac{\partial^2 \phi}{\partial x \partial y} \right] - p(x,y) - k_w(x,y) = 0$$

$$\nabla^4 \phi = E \left[\left(\frac{\partial^2 w}{\partial x \partial y} \right)^2 - \frac{\partial^2 w}{\partial x^2} \frac{\partial^2 w}{\partial y^2} \right] \quad (4.8)$$

In addition to the use of a discrete element model, which discussed in the following sections, the most important methods for solution of nonlinear plate problems are: integration of differential equations (exact solution), variational methods, finite different methods, iterative techniques, and numerical integration.

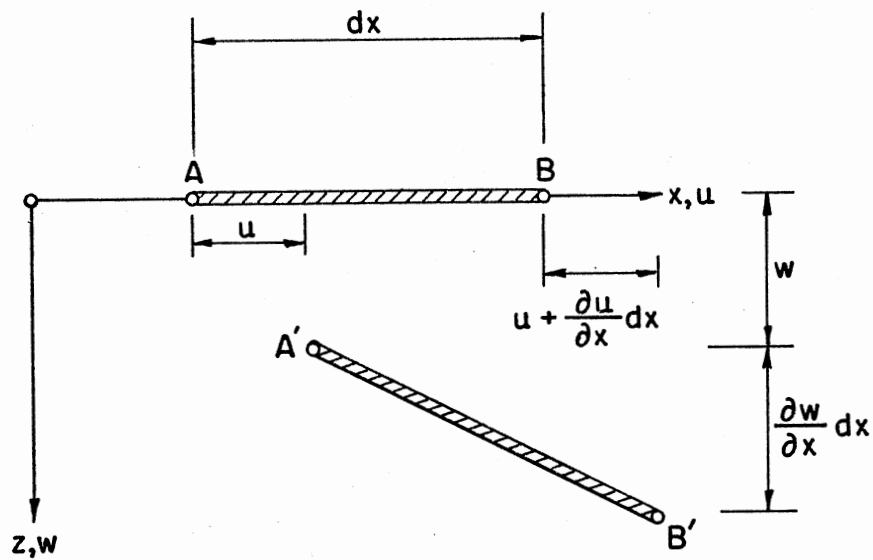


Figure 14. Strain, ϵ_x , Due to Large Deflections

4.3 Discrete Element Model

4.3.1 General

The general theory of plates discussed in the preceding articles are based on infinitesimal calculus. Close-form solutions for the large deflection problem, and for the majority of complex engineering problems, are not available. Numerical methods are most often used to solve complex engineering problems, in which the governing differential equations can be mathematically approximated by the substitution of finite difference form for derivatives. Numerical methods are applied using a physical model, in which the problem is represented by a system of finite or discrete elements whose behavior can properly be described with algebraic equations. The physical model facilitates visualization of the problem and the formulation of proper boundary and loading conditions.

In this study a discrete element model developed by Hrennikoff (13) will be used.

4.3.2 Membrane Model

The model shown in Figure 15 is utilized to represent the membrane behavior of the plate. This model is composed of ball and socket joints and elastic bars. The elastic bars transmit membrane forces by stretching and contracting. The properties of elastic bars and the strain relation between bars and plates are discussed in Appendix A. The stiffness matrix for the membrane resembles that of the space truss and has been presented by Przemieniecki (19).

The equilibrium equations of this membrane model are summarized into matrix form as

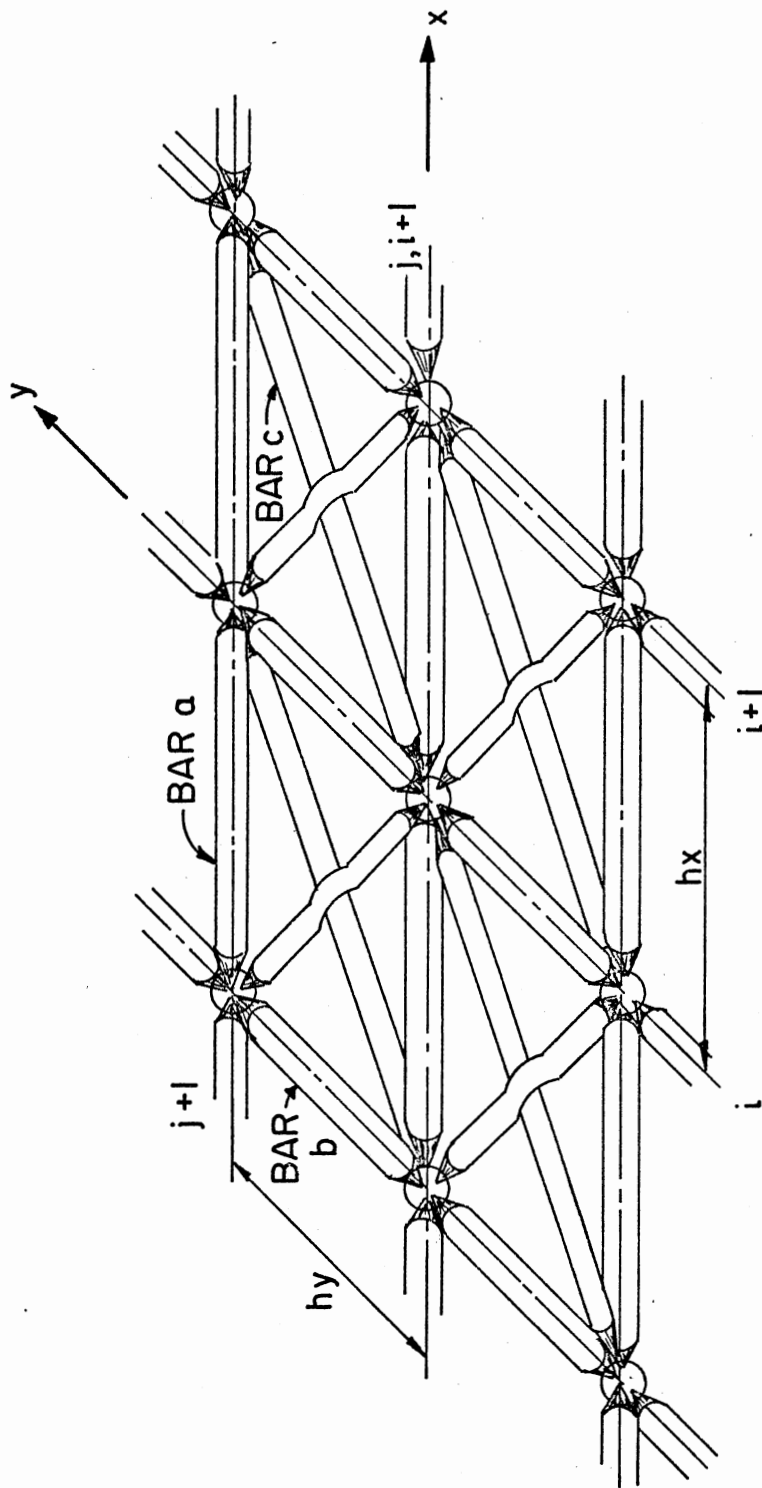


Figure 15. Membrane Model

$$[S]\{u\} = \{F\} \quad (4.9)$$

where

$[S]$ = stiffness matrix for the membrane model;

$\{u\}$ = displacement vector of the membrane model i ; and

F = force vector of the membrane model.

4.3.3 Model Stress Resultant

Membrane stresses are calculated from the forces in the elastic bars of the membrane model. Bar forces are calculated from the vertical and in-plane displacements of the membrane model, as discussed in Appendix A. Membrane stresses are expressed as:

$$\begin{aligned} \sigma_x &= [F_A + F_B + (F_H + F_E) \cos\theta]/th_y \\ \sigma_y &= [F_C + F_D + (F_y + F_E) \sin\theta]/th_x \\ \tau_{xy} &= [F_H + F_E] \cos\theta/th_x \\ \tau_{yx} &= [F_H + F_E] \sin\theta/th_x \end{aligned} \quad (4.10)$$

where σ_x, σ_y are normal membrane stresses; τ_{xy}, τ_{yx} are membrane shearing stresses; and $F_A, F_B, F_C, F_D, F_E,$ and F_H are forces in elastic bars of the model (see Figure 15). The derivation of Equation (4.10) is given in Appendix A.

4.4 Nonlinear Analysis

Since the fabric is horizontal before the application of the vertical loads, its membrane resistance is zero. To overcome this difficulty, a very small bending rigidity will be assumed and a very small part of the load will be applied first. It will cause the fabric (plate) to

deflect and membrane resistance will be mobilized. Equilibrium, then, is evaluated by calculation of the vertical and in-plane resistance of the membrane model. If equilibrium is not satisfied, the joint deflection is adjusted and the equilibrium equation is checked again. In other words, the solution is obtained by an iteration technique in which static equilibrium of the joints of the model is achieved.

CHAPTER V

DESIGN PROCEDURE

5.1 General

It is important in any design problem to provide a practical way to satisfy design criteria. To develop this the mechanical behavior must be postulated. Since the interaction between fabrics and soil is not fully known, it is necessary to assume mechanisms which are believed to resemble those of the actual interaction.

In this section some design assumptions will be suggested for different soil mechanics problems.

5.2 Footing Design

5.2.1 General

It has been shown that the fabric below a footing acts like a plate with no bending rigidity and, hence, the more the membrane displaces vertically from its initial position the more vertical resistance it will mobilize. This can be shown by comparing the improvement factor for different settlement ratios corresponding to the same depth ratio (16).

For this reason it is reasonable to start design (or check of stresses) by choosing the maximum allowable vertical displacement.

5.2.2 Suggested Design Procedure

Let us assume that it is required to design the isolated footing shown in Figure 17. The procedure is as follows:

1. First of all, the depth ratio should be assumed. As shown in Figure 16(b), it is desirable for the depth ratio to be between 0.4 and 0.6 (16), to effect the greatest improvement in performance.

2. Next it is necessary to assume a certain displacement configuration for the fabric membrane. Let us assume the deflection surface, shown in Figure 18, described as follows:

$$0 < x, y < na$$

$$\frac{x^2}{(na)^2} + \frac{y^2}{(na)^2} = \frac{z}{r\Delta_0} \quad (5.1)$$

$$na < x, y < A$$

$$\frac{x^2}{(na)^2} + \frac{y^2}{(na)^2} + \left(\frac{2r\Delta_0}{C_1(na)^3} - \frac{2}{na}\right)x + \left(\frac{2r\Delta_0}{C_1(na)^3} - \frac{2}{na}\right)y - \frac{z}{C_2} = C_3$$

where

$$C_1 = \frac{\Delta_0}{(A - na)^2} \left[1 - r - \frac{2rA}{na}\right]$$

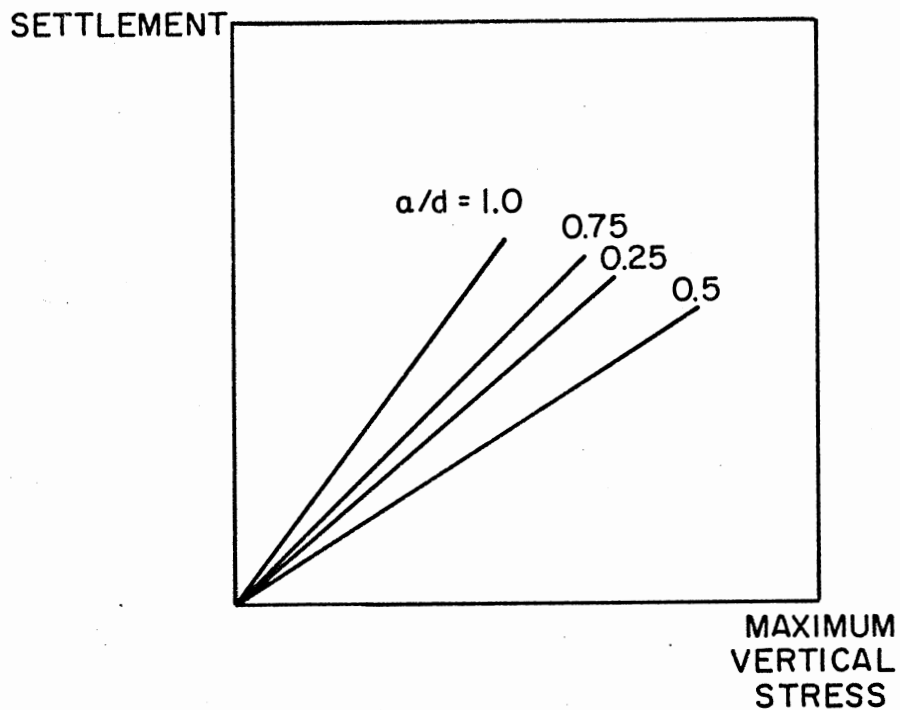
$$C_2 = (na)^2 C_1$$

$$C_3 = [r\Delta_0 - C_1(na)^2 - C_2(na)] / (na)^2 C_1$$

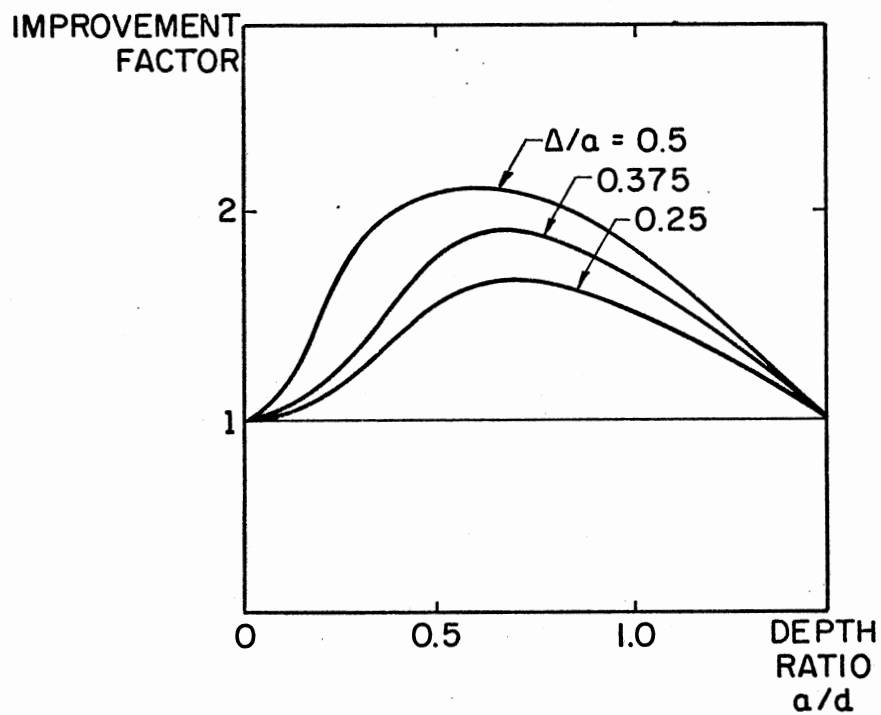
3. Utilize an expression for static equilibrium to obtain the minimum lateral dimensions of the fabric inclusion.

$$\Sigma F_2 = 0$$

$$P = KV$$



(a) Effect of Depth Ratio (a/d) on a Stress-Settlement Relation (16)



(b) Effect of Maximum Allowable Settlement Δ on the Improvement Factor (16)

Figure 16. Factors Affecting Fabric Usefulness

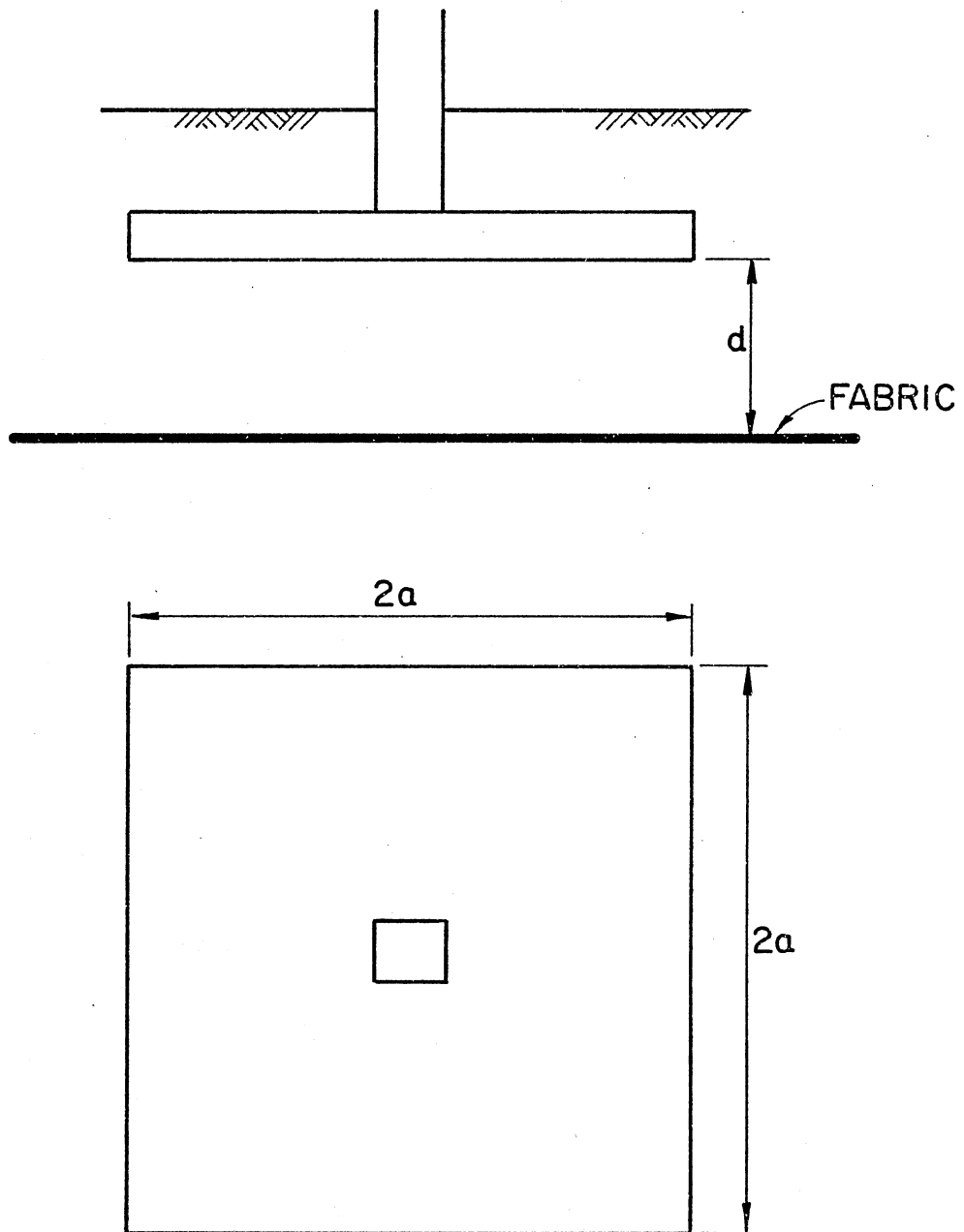


Figure 17. Reinforced Footing Foundation

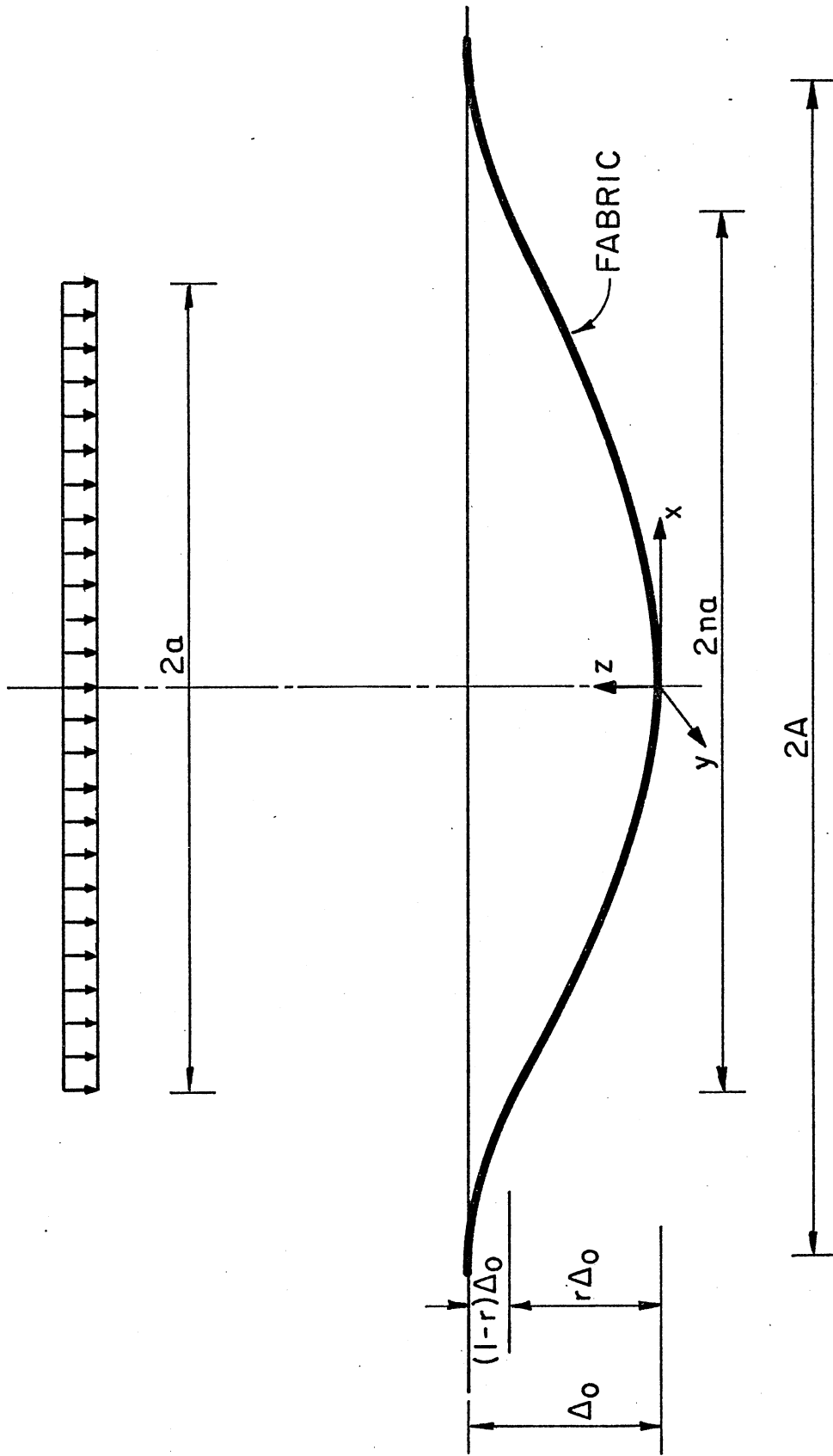


Figure 18. Deformed Fabric Under Footing Load

where K is the coefficient of subgrade reaction, and V is volume between deformed and undeformed positions of the fabric. Substituting for V , we get

$$P = \frac{\pi K \Delta_0}{6} [2(na)^2 (3+r) + (1-r) (A - na) (A + 3na)] \quad (5.2)$$

Several problems were solved using the method explained in Chapter IV, and it was concluded that the following values for n and r can be assumed without introducing significant error.

$$r = 0.65 \text{ to } 0.8$$

$$n = 1.00$$

Substituting these values for r and n , the unknown value of A can be obtained from Equation (5.2).

4. After determining the required dimension of the fabric, tension in the membrane needs to be checked. Considering Figure 19 and writing the equilibrium equation in the vertical direction, we get

$$T(2\pi a) \sin\theta = \left(\frac{\pi}{6}\right) (K) (\Delta_0) (1-r) (A - a) (A + 3a)$$

Since θ is small,

$$\sin\theta = \tan\theta = \frac{2\Delta_0}{a}$$

Substituting into the above equation, we get

$$T = \frac{K}{80} (A - a) (A + 3a) \quad (5.3)$$

5.3 Slope Stability

5.3.1 General

It was mentioned in Chapter II that Christie and Hadi (7) considered

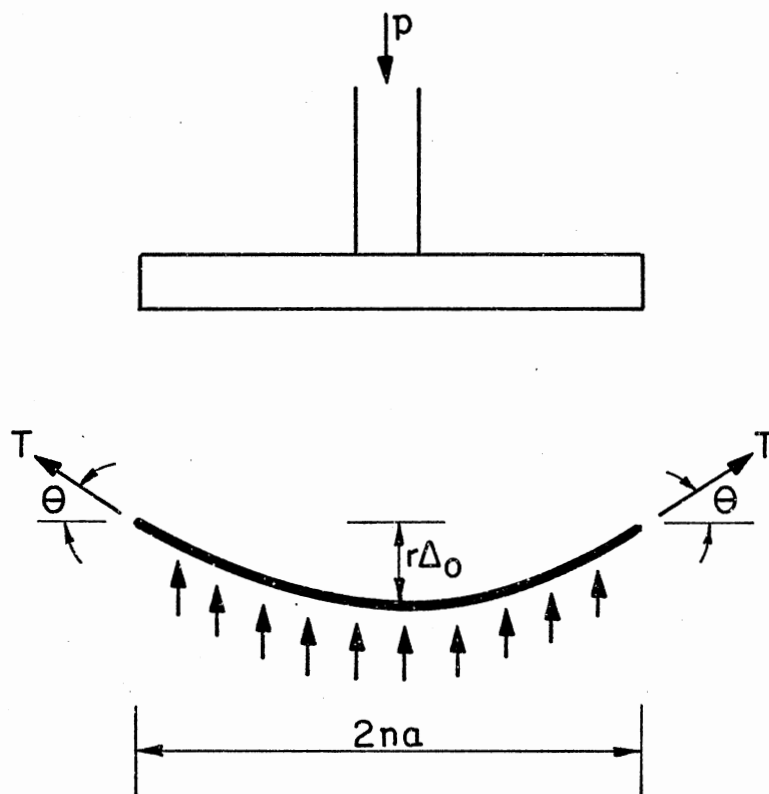


Figure 19. Free Body Diagram for Deformed Fabric

an embankment reinforced with horizontal fabric membranes using conventional slices method. Fawzy (9) proposed using radial reinforcement to mobilize maximum stabilizing moment. However, neither one considered membrane deformation which is the cornerstone of fabric-soil interaction. Again, that is because the resistance that will be offered by the membrane is proportional to its vertical displacement. In this section vertical displacement of the membrane will be investigated, and a correlation between fabric deformation and design aspects will be obtained.

5.3.2 Design Criteria

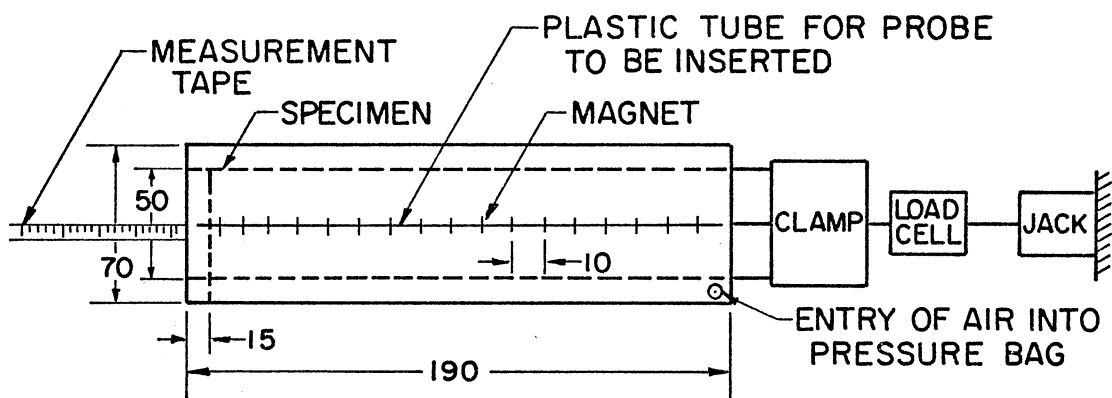
In an isolated footing analysis, a displacement criterion should be determined before going into design steps. It is more convenient to consider a relative displacement between elements along the perimeter of the slip circle (see Figure 21). It will be assumed that there is a permissible maximum relative displacement of Δ_0 along the slip circle, and that no slippage is permitted between fabric and the surrounding soil.

5.3.3 Pullout Test

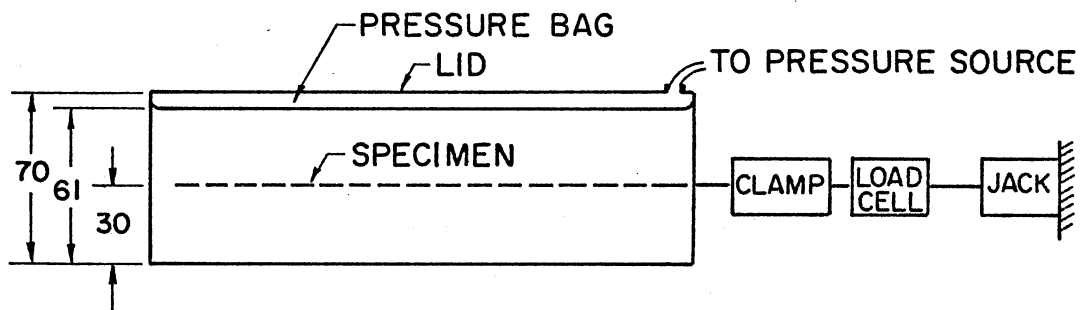
A pullout test should be performed in order to calculate the resistance coefficient, ρ_r , which represents the friction force per unit length of the surface (see Appendix B).

The apparatus to be used is shown in Figure 20. A complete discussion is given by Holtz (3). To find the magnitude of the pullout force T that is compatible with the design displacement Δ_0 , the following relation will be assumed.

$$\frac{u_0}{\Delta_0} = \frac{T_L}{T_F} \quad (5.4)$$



(a) TOP VIEW



(b) SIDE VIEW

NOTE: ALL DIMENSIONS IN CM.

Figure 20. Pullout Test Apparatus

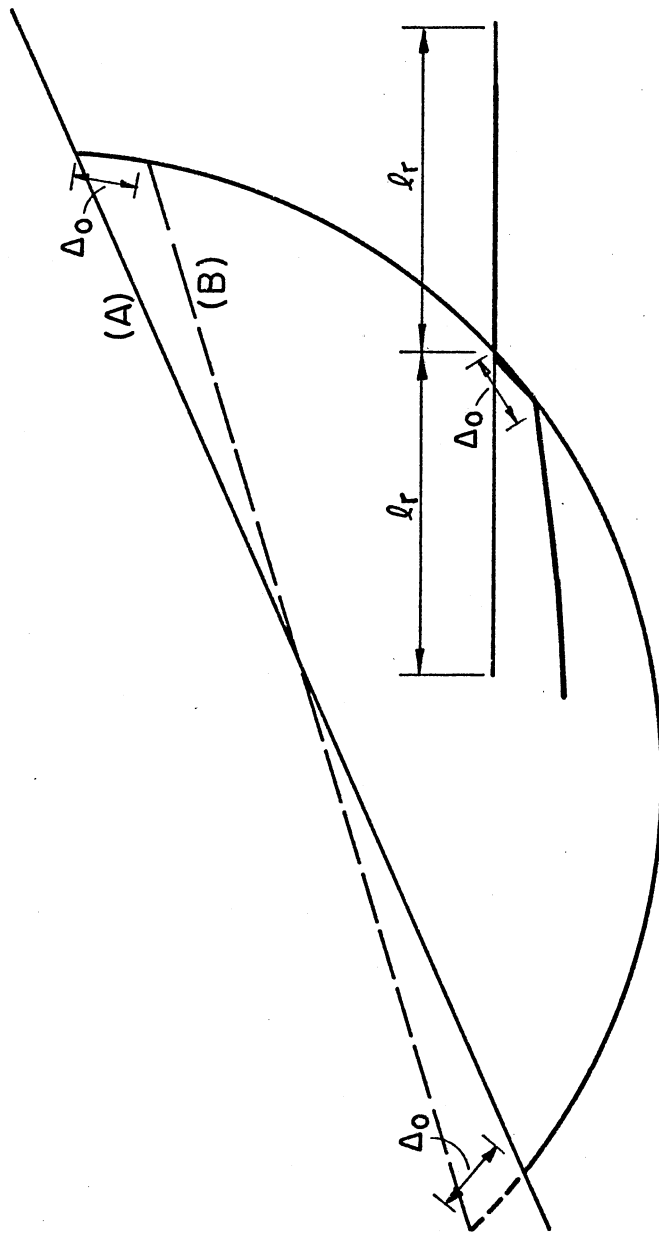


Figure 21. Deformed Fabric in Slope Stability Problem

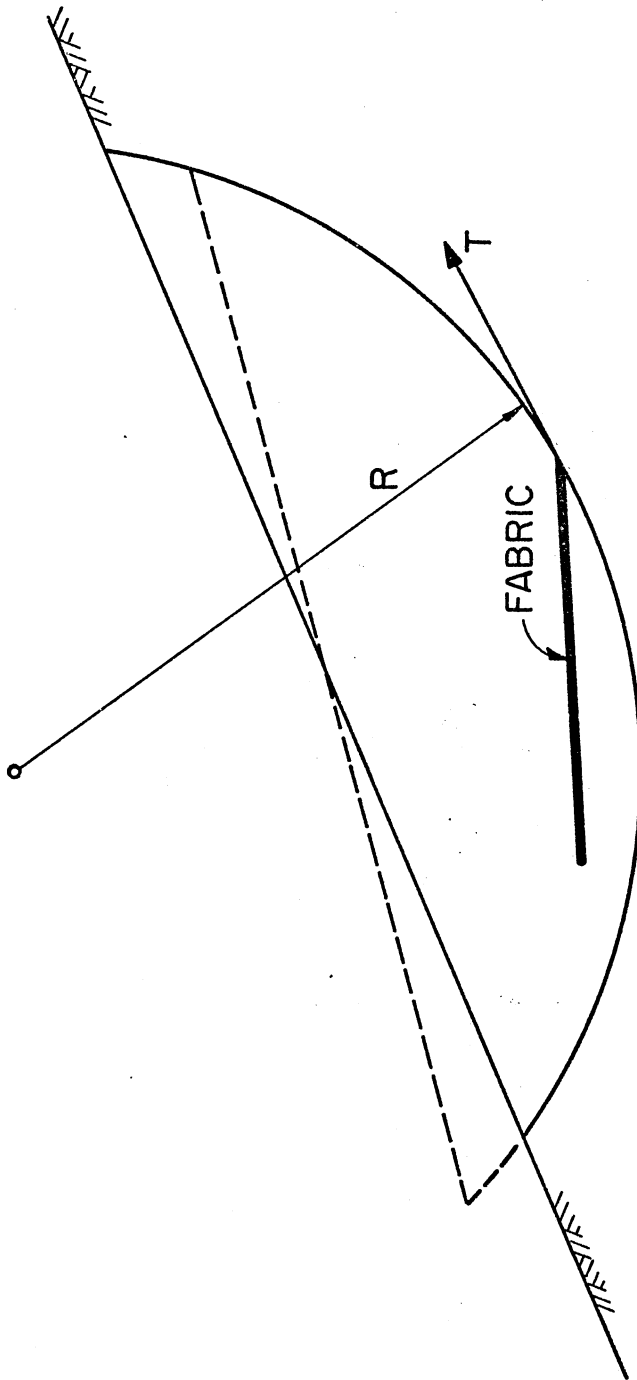


Figure 22. Free Body Diagram for the Sliced Mass

where

u_0 = displacement of the strip tested in the laboratory;

Δ_0 = design displacement;

T_L = pullout force measured in the pullout test; and

T_F = force compatible with the design displacement, Δ_0 .

5.3.4 Design Steps

The following design steps should be followed:

1. Conduct a pullout test and calculate ρ_r .
2. Assume a reasonable value for Δ_0 .
3. Using Equation (5.4), find the corresponding T_F .
4. Design the minimum anchorage length as given in Appendix B.

5.3.5 Equilibrium

It is interesting to note that the fabric membrane resisting force, T , will not be mobilized before some deformation occurs. This implies that the fabric will be ineffective if it has been placed in a "safe" embankment.

Let us assume that the slice method of analysis (without fabric reinforcement) has led to a factor of safety $F_1 < 1.0$, and it is required that it be improved to a factor of safety F_2 using fabric reinforcement. Thus the required additional stabilizing moment is

$$M_{sf} = (F_2 - F_1) M_D \quad (5.5)$$

where M_{sf} is the stabilizing moment mobilized as a result of fabric inclusion, and M_D is the driving moment. Referring to Figure 21, it can be readily seen that for n sheets of fabric placed in the embankment,

$$M_{sf} = \sum_1^n T_i R \quad (5.6)$$

Provided that the resulting T does not exceed the strength of the fabric, the required factor of safety will be provided if the length of anchorage is sufficient.

CHAPTER VI

UNCERTAINTY AND PROBABILISTIC DESIGN

6.1 General

In soil mechanics, as in any physical problem of interest, there is an element of uncertainty, unpredictability, or randomness associated with the variations in the physical properties of soil. For example, no matter how many samples were tested in consolidation, it is almost impossible to predict exactly the settlement behavior of a soil mass.

In the reinforced earth problem there are different degrees of certainty involved in defining the pertinent physical properties of the soil and of the reinforcement. This suggests that there is an element of probability associated with the design, and that design procedures could be adopted which take this into account. That is, it is possible to state the probability with which a predicted result will fall within a specified range of results.

Although the analytical method recommended as the principal result of this study is not a probabilistic one, it is useful to provide the background for making such an analysis, and to present a simple numerical example related to soil properties. Properties such as strength, density, water content, compressibility, etc. are assumed to follow a normal distribution.

6.2 Gaussian Distribution

If X_1, X_2, \dots, X_n are the results of tests on random samples, where X_i indicates the result of the i^{th} experiment (for instance, cohesion, compression index, etc.), and the samples have been taken from a population which has a normal (Gaussian) distribution $n(\theta, \sigma^2)$, as indicated in Figure 23, where θ is the mean, σ^2 is the variance, and

$$f(X_i, \theta) = \frac{1}{\sqrt{2\pi\sigma^2}} e^{-\frac{1}{2\sigma^2} (X_i - \theta)^2} \quad (6.1)$$

6.3 Estimation

Suppose it is agreed that a certain soil characteristic, say relative density, is a random variable, and that it follows a normal distribution. It is now necessary to estimate the relative density, D_r , with some specified degree of reliability. There are two main approaches to estimate the expected relative density: the classical statistical solution which considers the mean (expected relative density) to be a constant, and a modern solution (Bayesian Solution) which treats the mean itself as a random variable. In this study, the second approach will be examined. This approach takes into account any prior knowledge of the property under consideration.

As mentioned before, let us consider a random variable D_r that has a distribution of probability that depends upon the symbol θ , where θ is an element of a well-defined set r . If the symbol θ is the mean of a normal distribution, Ω may be the real line. The probability density function (p.d.f.) of θ shall be denoted $h(\theta)$, and $h(\theta) = 0$ when θ is not an element of Ω . Let $D_{r1}, D_{r2}, D_{r3}, \dots, D_{rn}$ denote the relative

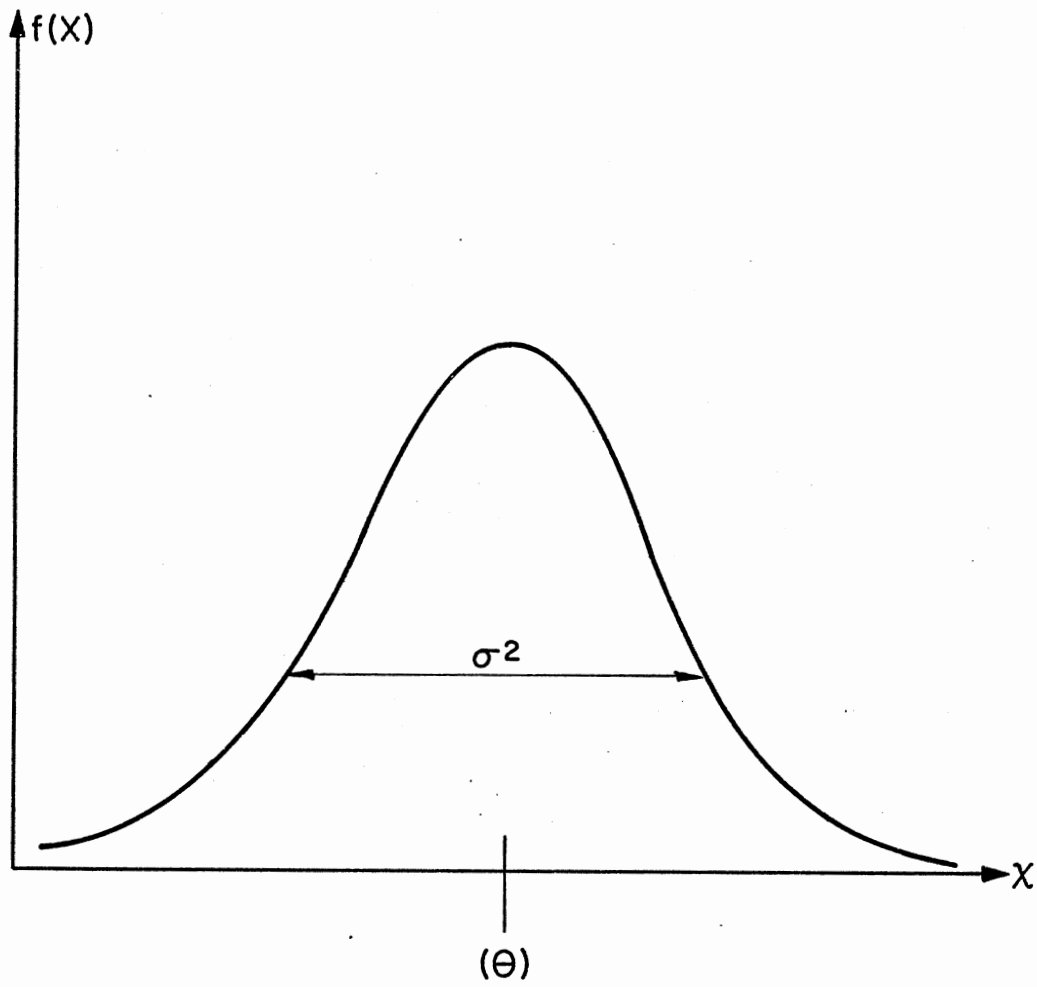


Figure 23. Gaussian Distribution Curve

densities of random samples from this distribution of D_r , and let Y denote a statistic that is a function of $D_{r1}, D_{r2}, \dots, D_{rn}$. The p.d.f. of Y can be found for every given θ ; that is, the conditional p.d.f. of Y can be found, given $\theta = \theta^*$ which will be denoted by $g(y/\theta)$. Thus the joint p.d.f. of Y and θ is given by

$$k(\theta, y) = h(\theta) g(y/\theta) \quad (6.2)$$

As θ is a random variable of the continuous type, the marginal p.d.f. of Y is given by

$$k_1(y) = \int_{-\infty}^{\infty} h(\theta) g(y/\theta) d(\theta) \quad (6.3)$$

The conditional p.d.f. of θ given $Y = y$ is

$$k(\theta/y) = \frac{k(y, \theta)}{k_1(y)} = \frac{h(\theta) g(y/\theta)}{k_1(y)} \quad (6.4)$$

In Bayesian statistics, the p.d.f. $h(\theta)$ is called the prior p.d.f. of θ , and the conditional $k(\theta/y)$ is called the posterior p.d.f. of θ . This is because $h(\theta)$ is the p.d.f. of θ prior to the observation of Y , whereas $k(\theta/y)$ is the p.d.f. of θ after the observation of Y has been made. In many instances $h(\theta)$ is not known, yet the choice of $h(\theta)$ affects the p.d.f. $k(\theta/y)$. In these instances one should take into account all prior knowledge of the property and assign the prior p.d.f. $h(\theta)$. This, of course, injects the problem of personal bias or subjective judgment. Define $w(y)$ to be that function of the observed value of the statistic Y which is the estimate of θ and let $w(g)$ be called a decision function. A decision may be correct or it may be wrong, and it would be useful to have a measure of the seriousness of the difference, if any, between the true value of θ and the estimate $w(g)$. Accordingly, with each pair, $[\theta, w(y)]$, $\theta \in \Omega$, we associate a non-negative number

$L[\theta, w(y)]$ that reflects this seriousness. We call the function L the loss function. The expected (mean) value of the loss function is called the risk function, stated as follows

$$R(\theta, w(y)) = E\{L[\theta, W(Y)]\} \quad (6.5)$$

In general, how would an experimental value of any random variable, say W , be predicted if the prediction is to "reasonably close" to the value to be observed? Many statisticians would predict the mean, $E(W)$, of the distribution W ; others would predict a median (perhaps unique) of the distribution of W ; some would predict a mode (perhaps unique) of the distribution W ; and some would have other predictions. However, it seems desirable that the choice of the decision function should depend upon the loss function $L[\theta, w(y)]$. One way in which this dependence upon the loss function can be reflected is to select the decision function w in such a way that the conditional expectation of the loss is a minimum. A Bayesian solution is a decision function that minimizes

$$E\{L[\theta, w(y)]/Y = y\} = \int_{-\infty}^{\infty} L[\theta, w(y)] K(\theta/y) d\theta \quad (6.6)$$

The conditional expectation of the loss, given $Y = y$, defines a random variable that is a function of the statistic Y . The expected value of that function of Y is given by

$$\begin{aligned} & \int_{-\infty}^{\infty} \left\{ \int_{-\infty}^{\infty} L[\theta, w(y)] k(\theta/y) d\theta \right\} k_1(y) dy \\ & = \int_{-\infty}^{\infty} \int_{-\infty}^{\infty} L[\theta, w(y)] g(y/\theta) dy \} h(\theta) d\theta \end{aligned} \quad (6.7)$$

The integral within the braces in the latter expression is, for every given $\theta \in \Omega$, the risk function $R(\theta, w(y))$; accordingly, the latter expression is the mean value of the risk, or the expected risk. Because the Bayesian solution minimizes

$$\int_{-\infty}^{\infty} L[\theta, w(y)] k(\theta/y) d\theta$$

for every y for which $k_1(y) > 0$, it is evident that a Bayesian solution $w(y)$ minimizes this mean value of the risk.

6.3.1 Example

Let C_1, C_2, \dots, C_n denote the cohesion of random samples from a distribution that is $n(\theta, \sigma^2)$, $-\infty < \theta < \infty$. Let $Y = \bar{C}$, the mean of the random sample distribution. θ is an observed value of the random variable θ that is normally distributed (μ, τ^2) , where τ^2 and μ are known numbers. If it is required to find the Bayesian solution $w(y)$ for a point estimate of θ , the loss functions should be known. Two different loss functions will be assumed.

$$1. L_1(\theta, w_1(y)) = [\theta - w(y)]^2$$

$$2. L_2(\theta, w_2(y)) = |\theta - w(y)|$$

The Bayesian solution $w(y)$ is that which minimizes the risk function.

Since

$$f(C_i/\theta) = \frac{1}{\sqrt{2\pi}\sigma} e^{-\frac{1}{2\sigma^2} (C_i - \theta)^2}$$

$$f(C_1, C_2, \dots, C_n/\theta) = \left(\frac{1}{\sqrt{2\pi}\sigma}\right)^n e^{-\sum \frac{1}{2\sigma^2} (C_i - \theta)^2} = g(y/\theta)$$

$$k(\theta/y) = \frac{h(\theta) g(y/\theta)}{k_1(y)} = C(y) h(\theta) g(y/\theta),$$

where

$$C(y) = 1/k_1(y),$$

$$\begin{aligned}
&= C(y) \frac{1}{2\pi\tau} e^{-\frac{1}{2\tau^2}(\theta - \mu)^2} \cdot e^{-\frac{1}{2\sigma^2} \sum [(C_i - \bar{C}) - (\theta - C)]^2} \\
&= C(y) e^{-\frac{1}{2\tau^2}(\theta - \mu)^2} e^{-\frac{1}{2\sigma^2} [\sum (C_i - \bar{C})^2 + n(\theta - \bar{C})^2]} \\
&= C(y) e^{-\frac{\theta^2}{2\tau^2} + \frac{\theta\mu}{\tau^2}} \cdot e^{-\frac{n\theta^2}{2\sigma^2} + \frac{n\theta\bar{C}}{\sigma^2}} \\
&= C(y) e^{\theta^2[-\frac{1}{2\tau^2} - \frac{n}{2\sigma^2}] + \theta[\frac{\mu}{\tau^2} + \frac{n\bar{C}}{\sigma^2}]} \\
&= C(y) e^{-\frac{1}{2}(\frac{1}{\tau^2} + \frac{n}{\sigma^2})[\theta^2 - \frac{\frac{\mu}{\tau^2} + \frac{n\bar{C}}{\sigma^2}}{\frac{1}{2\tau^2} + \frac{n}{2\sigma^2}}\theta]} \\
&= C(y) e^{-\frac{1}{2}(\frac{1}{\tau^2} + \frac{n}{\sigma^2})[\theta - \frac{\frac{\mu}{\tau^2} + \frac{n\bar{C}}{\sigma^2}}{\frac{1}{\tau^2} + \frac{n}{\sigma^2}}]^2} \\
(1) \quad K(\theta/y) &= n \left(\frac{\frac{\mu}{\tau^2} + \frac{n\bar{C}}{\sigma^2}}{\frac{1}{\tau^2} + \frac{n}{\sigma^2}}, \frac{1}{\frac{1}{\tau^2} + \frac{n}{\sigma^2}} \right)
\end{aligned}$$

First, consider loss function number (1). It can be shown that $w(y) = E(\theta/y)$ minimizes the risk function. Hence the Bayesian Solution is $E(\theta/y)$, where

$$(2) \quad E(\theta/y) = \frac{\frac{\mu}{\tau^2} + \frac{n\bar{C}}{\sigma^2}}{\frac{1}{\tau^2} + \frac{n}{\sigma^2}}$$

Second, consider loss function number (2). It can be shown that $w(y) = \text{median}(\theta/y)$ also minimizes the risk function, but since $K(\theta/y)$

is a normal distribution function, the median is equal to the mean, and

$$(3) \quad w(y) = \frac{\mu}{\tau^2} + \frac{n\bar{C}}{\sigma^2}.$$

6.3.2 Remarks

The following remarks apply:

1. The conditional posterior mean $E(\theta/y)$ is a linear combination of the prior mean (μ) and the sample mean \bar{C} .

2. The first term (μ/τ^2) indicates the confidence of the prior assumption; that is, if one is confident about the prior assumption μ , this term will contribute to $E(\theta/y)$ more than the second term ($n\bar{C}/\sigma^2$), because τ^2 will get smaller as confidence in μ increases. If we are certain about (μ), then $\tau^2 \rightarrow 0$ and $E(\theta/y) \rightarrow \mu$.

3. The second term indicates the contribution of the sample to the estimate. Hence, if the prior assumption (μ) is not close enough or τ^2 is big, the second term plays the main role in estimation. In other words, as $\tau^2 \rightarrow \infty$, $E(\theta/y) \rightarrow \bar{C}$.

A complete numerical example is given in Appendix C.

CHAPTER VII

CASE STUDY

7.1 Statement and Description of the Problem

The general location of an embankment test section described by Haliburton, Douglas, and Fowler (22) is shown in Figure 24. As may be noted in the figure, the test section was constructed across an intertidal area, with existing ground elevations over most of the alignment ranging between El. 1.5 Mean Sea Level (MSL) and El. -1.0 MSL.

7.2 Embankment-Foundation Data

The embankment was constructed of Mobile Sand, a fine, poorly graded, semi-angular, fairly clean material with 100 percent passing the U.S. No. 10 sieve, 83 percent passing the U.S. No. 40 sieve, and 2 percent passing the U.S. No. 100 sieve, with a uniformity coefficient of 1.3. This material may be classified SP by the Unified Soil Classification System. These data were obtained from samples taken at the borrow area location shown in Figure 24.

The sand was placed in the embankment in a loose relative density state, for which the friction angle ϕ is assumed to be 30 degrees.

The unit weight of the embankment material is taken as 100 pcf above the permanent water table and 60 pcf below the permanent water table, with the latter value used in computing effective bearing pressures for future dike raising after foundation consolidation and

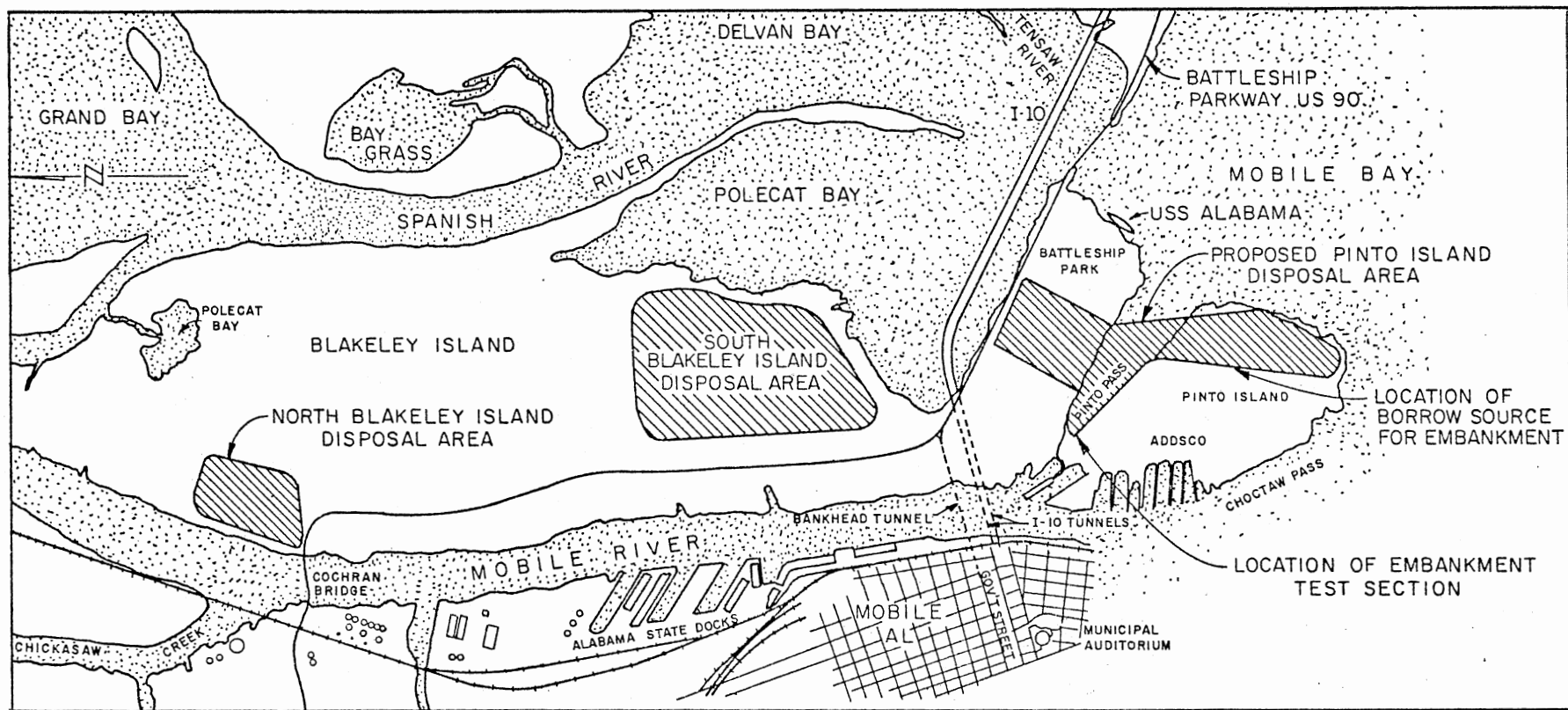


Figure 24. General Location of Embankment Test Section in Mobile Harbor, Alabama

settlement. The permanent water table was assumed to exist at El. 0.0 MSL.

Based on the results of field vane shear tests and strength tests conducted by the Soils and Pavements Laboratory (U.S. Army Engineer Waterways Experiment Station [WES], Vicksburg, Mississippi) on undisturbed samples of foundation material at the west end of Pinto Pass, assumed minimum unconsolidated, undrained (Q) soil strength conditions at the time of test section construction consisted of material with $\phi = 0$, C - 50 psf from the surface to El. -10 MSL, $\phi = 0$, C - 100 psf from El. -10 MSL to El. -20 MSL, and $\phi = 0$, C - 150 psf from El. -20 MSL to El. -40 MSL, where medium-dense to dense clean sand is found. In predicting available foundation strength for future dike raising, results of consolidated undrained (R) shear strength tests conducted by the WES on the material indicated a cohesion of 0.15 and a friction angle ϕ of 11 degrees.

7.3 Fabric Data

In their evaluation of civil engineering fabric for use as embankment reinforcement, Haliburton, Anglin, and Lawmaster (23) recommended four civil engineering fabrics: Nicolon 66475, Nicolon 66186, Advance Type I, and Polyfilter-X, plus one fiberglass fabric, Bay Mills 196-380-000.

Test data for these five fabrics developed from Reference (23) are summarized in Table I.

TABLE I
SUMMARY OF FABRIC WRAP DIRECTION
LABORATORY TEST RESULTS

Fabric	Tensile Stress at 10%E lb/in.-width	Ultimate Tensile Stress lb/in.-width	Creep Tendency	Wet Strength Loss
Nicolon 66475	362	902	Nil	Nil
Nicolon 66186	109	226	Nil	Nil
Polyfilter-X	103	311	Moderate	High
Advance Type I	108	252	High	Moderate
Bay Mills 196-380-000	318 (8%E)	318	Zero	Not Tested

TABLE II
TYPE AND LOCATION OF FABRIC REINFORCEMENT
IN EMBANKMENT

Place North Edge of Fabric Strip at Station	Fabric To Be Used	Place North Edge of Fabric Strip at Station	Fabric To Be Used
0+60	Advance Type I	4+20	Nicolon 66475
0+75	Advance Type I	4+35	Nicolon 66475
0+90	Advance Type I	4+50	Nicolon 66475
1+05	Advance Type I	4+65	Nicolon 66475
1+20	Advance Type I	4+80	Nicolon 66475
1+35	Advance Type I	4+95	Nicolon 66475
1+50	Advance Type I	5+10	Nicolon 66475
1+65	Advance Type I	5+25	Nicolon 66475
1+80	Advance Type I	5+40	Nicolon 66475
1+95	Advance Type I	5+55	Nicolon 66475
2+10	Advance Type I	5+70	Nicolon 66475
2+25	Advance Type I	5+85	Nicolon 66475
		6+00	Nicolon 66475
2+40	Polyfilter-X	6+15	Nicolon 66475
2+55	Polyfilter-X	6+30	Nicolon 66475
2+70	Polyfilter-X	6+45	Nicolon 66475
2+85	Polyfilter-X		
3+00	Polyfilter-X	6+60	Nicolon 66186
3+15	Polyfilter-X	6+75	Nicolon 66186
3+30	Polyfilter-X	6+90	Nicolon 66186
3+45	Polyfilter-X	7+05	Nicolon 66186
3+60	Polyfilter-X	7+20	Nicolon 66186
3+75	Polyfilter-X	7+35	Nicolon 66186
3+90	Polyfilter-X	7+50	Nicolon 66186
4+05	Polyfilter-X	7+65	Nicolon 66186
		7+80	Nicolon 66186
		7+95	Nicolon 66186
		8+10	Nicolon 66186

NOTE: All fabric strips 200 ft long.
Polyfilter-X and Advance Type I 18 ft wide, 1.5-ft overlap
at each end.
Nicolon 66186 and 66475 16.4 ft (5 m) wide, 0.7-ft overlap
at each end.

7.4 Location of Fabric in Embankment

The following data describe the location of the various fabrics in the embankment: Advance Type I fabric is used for reinforcement from embankment Sta 0+60 to Sta 2+40; Polyfilter-X fabric from Sta 2+40 to Sta 4+20; Nicolon 6675 fabric from Sta 4+20 to Sta 6+45; and Nicolon 66186 fabric from Sta 6+45 to Sta 8+00. Table II gives the specific installation instructions.

7.5 Results of Analysis

Because of a lack of data, the following assumptions were used in the analysis (Table III).

TABLE III
ASSUMPTIONS USED IN ANALYSIS

Fabric Type	$\rho_r \times 10^{-3}$ (kip/ft)	U_0	U'_0	T_L (kip/ft)
Advance Type I	30	0.25	0.05	0.73
Polyfilter-A	30	0.27	0.05	0.71
Nicolon 66475	30	0.12	0.05	0.91
Nicolon 66186	30	0.26	0.05	0.82

The analysis described in Chapter V yields the following results (Table IV).

TABLE IV
RESULTS OF ANALYSIS

Fabric Type	Δ_0 (in.)	Estimated Safety Factor
Advance Type I	0	0.92
	5	0.97
	10	1.09
	15	1.27
	20	1.62
Polyfilter-X	0	0.92
	5	0.95
	10	1.03
	15	1.18
	20	1.53
Nicolon 66475	0	0.92
	5	1.03
	10	1.25
	15	1.74
	20	2.11
Nicolon 66186	0	0.92
	5	0.94
	10	1.07
	15	1.21
	20	1.57

The expected deformations are those corresponding to a safety factor of 1.0. Those deformations obtained by interpolation from the above results are:

1. Advance type I: $\Delta_0 = 7.8$ in.
2. Polyfilter-X: $\Delta_0 = 8.8$ in.
3. Nicolon 66475: $\Delta_0 = 4.1$ in.
4. Nicolon 66186: $\Delta_0 = 7.4$ in.

The observed deformations were:

1. Advance type I: $\Delta_0 = 7.1$ in.
2. Polyfilter-X: $\Delta_0 = 7.8$ in.
3. Nicolon 66475: $\Delta_0 = 3.9$ in.
4. Nicolon 66186: $\Delta_0 = 6.8$ in.

7.6 Conclusions

The following can be concluded from the previous article:

1. The four reaches are safe, and have probably deformed to a stable configuration.
2. The embankment would have failed without reinforcement.
3. The proposed method of prediction produced results that are in very good agreement with the observed behavior of the only test embankment presently available for comparison.

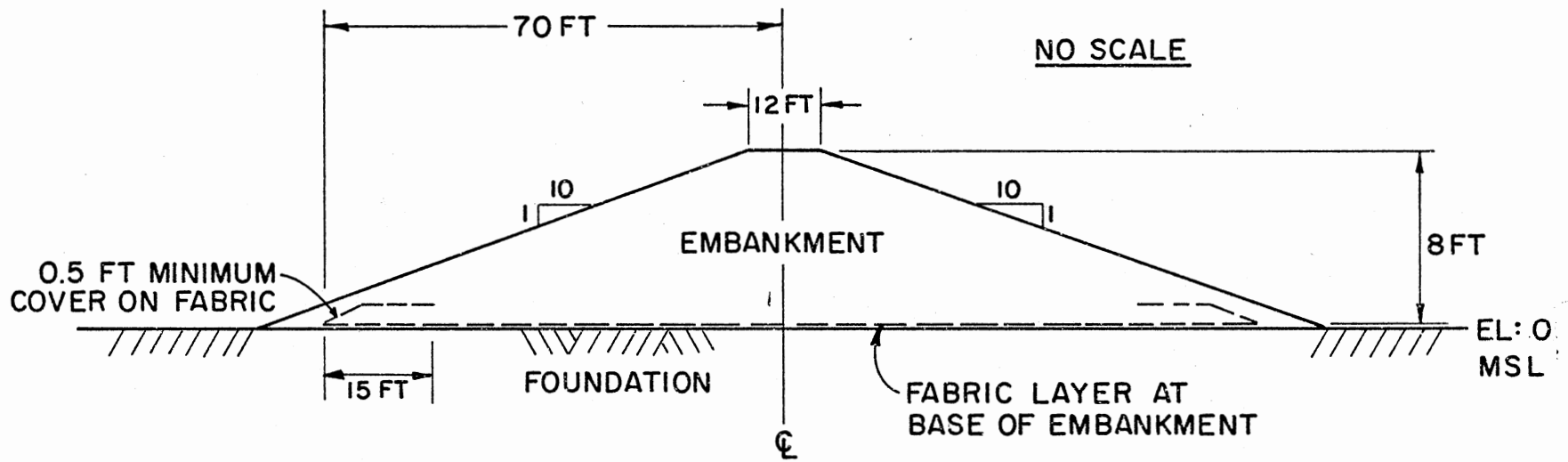


Figure 25. Simplified Fabric-Reinforced Embankment Section
Used for Analysis Purposes

CHAPTER VIII

SUMMARY AND RECOMMENDATIONS

A fabric membrane was modeled using the Hrennikoff model with no bending rigidity. It was shown that special provisions should be taken in order to enforce compatibility and simulate the no-tension property of soil when using the finite element method of analysis; however, this method was not used in the proposed method of analysis. The excellent agreement between the proposed method of analysis and the numerical solution explained in Chapter IV, and between the results of the analysis and the actual Alabama dike observations, implies that the design procedure suggested in Chapter V provides a practical and reliable way for solving a reinforced earth problem.

The mechanics of reinforced earth work discussed in Chapter II may be fully investigated either experimentally or analytically. The finite element methods seems to be appropriate for this purpose, but load tests on soil masses of different dimensions provides a reasonable way to estimate the dimensions of the soil mass that will be affected by the reinforcement.

The statistical model presented in Chapter VI is simple and fundamental, for it considers only soil parameters as random variables; hence, a more general model where the safety factor is considered a random variable as well needs to be explored.

REFERENCES

- (1) Al-Hussaini, M. M. "Field Experiment of Fabric Reinforced Earth Wall." International Conference on the Use of Fabrics in Geotechnics, Vol. 1, Paris (April, 1977), p. 119.
- (2) Barvashov, V. A. "Deformations of Soil Foundations Reinforced Earth Prestressed Synthetic Fabric." International Conference on the Use of Fabrics in Geotechnics, Vol. 1, Paris (April, 1977), p. 67.
- (3) Holtz, Robert D. "Reinforced Earthworks Mechanics." NSF Final Technical Report, Grant No. ENG 74-17810. Purdue University, May 31, 1978.
- (4) Bell, J. R. "Construction and Analysis of Fabric Reinforced Low Embankment on Muskeg." International Conference on the Use of Fabrics in Geotechnics, Vol. 1, Paris (April, 1977), p. 71.
- (5) Bell, J. R. "Construction and Observations of Fabric Retained Soil Wall." International Conference on the Use of Fabrics in Geotechnics, Vol. 1, Paris (April, 1977), p. 123.
- (6) Bakker, J. G. "Mechanical Behavior of Membranes in Road Foundations." International Conference on the Use of Fabrics in Geotechnics, Vol. 1, Paris (April, 1977), p. 139.
- (7) Christie, I. F. "Some Aspects of the Design of Earth Dams Reinforced With Fabric." International Conference on the Use of Fabrics in Geotechnics, Vol. 1, Paris (April, 1977), p. 99.
- (8) Eisenmann, J. "Experiments on the Use of Synthetic Non-Woven Materials of Road Structures." International Conference on the Use of Fabrics in Geotechnics, Vol. 1, Paris (April, 1977), p. 41.
- (9) Fawzy, A. "Soil Reinforcement With Fabrics." Unpublished paper submitted to the School of Civil Engineering, Oklahoma State University, Stillwater, Oklahoma, 1978.
- (10) Haliburton, T. A. "Soil Structure Interaction, Numerical Analysis of Beams and Beam Columns." Technical Publication No. 14. School of Civil Engineering, Oklahoma State University, Stillwater, Oklahoma, February, 1971.

- (11) Holtz, R. D. "Walls Reinforced by Fabrics--Results of Model Tests." International Conference on the Use of Fabrics in Geotechnics, Vol. 1, Paris (April, 1977), p. 113.
- (12) Holtz, R. D. "Reinforced Earthworks Mechanics." Technical report submitted to the National Science Foundation. Purdue University, May, 1978.
- (13) Hrennikoff, A. "Solution of Problems of Elasticity by the Frame Work Method." Journal of Applied Mechanics, ASME, Vol. 63 (December, 1941), p. A169.
- (14) Jessberger, H. L. "Load Bearing Behavior of Gravel Subgrade." International Conference on the Use of Fabrics in Geotechnics, Vol. 1, Paris (April, 1977), p. 9.
- (15) Maagdenberg, A. C. "Fabrics Below Sand Embankment Over Weak Soils." International Conference on the Use of Fabrics in Geotechnics, Vol. 1, Paris (April, 1977), p. 77.
- (16) McGown, A. "The Influence of Non-Woven Fabric Inclusion on Stress-Strain Behavior of a Soil Mass." International Conference on the Use of Fabrics in Geotechnics, Vol. 1, Paris (April, 1977), p. 161.
- (17) Nieuvenhuis, J. D. "Membranes and Bearing Capacity in Roadbases." International Conference on the Use of Fabrics in Geotechnics, Vol. 1, Paris (April, 1977), p. 3.
- (18) Love, A. E. H. The Mathematical Theory of Elasticity. 4th ed. Cambridge: Oxford University Press, 1927.
- (19) Przemieniecki, J. S. Theory of Matrix Structural Analysis. New York: McGraw-Hill Book Company, 1971.
- (20) Schwab, E. F. "Deformation Behavior of Reinforced Sand and Model Tests Measured by X-Ray Technique." International Conference on the Use of Fabrics in Geotechnics, Vol. 1, Paris (April, 1977), p. 105.
- (21) Szilard, R. Theory and Analysis of Plates. Englewood Cliffs, N.J.: Prentice-Hall, Inc., 1974.
- (22) Haliburton, T. A., P. A. Douglas, and J. Fowler. "Feasibility of Pinto Island as a Long-Term Dredged Material Disposal Site." Dredged Material Research Program, Report No. MP D-77-3. U.S. Army Engineer Waterways Experiment Station, Vicksburg, Mississippi, December, 1977.
- (23) Haliburton, T. A., C. C. Anglin, and J. D. Lawmaster. "Selection of Geotechnical Fabrics for Embankment Reinforcement." Contract No. DACW01-78-C-0055. U.S. Army Engineer District, Mobile, Alabama, May, 1978.

APPENDIX A

PROPERTIES OF MEMBRANE MODEL

Bar Cross-Sectional Areas

The in-plane behavior of a plate problem is represented by a membrane model shown in Figure 15. This membrane model is composed of elastic bars connected by ball and socket joints. The areas of these bars are related to the increment lengths, plate thickness and material properties. The evaluations of these areas are presented elsewhere (13), but are included in these work for the benefit of the reader.

The areas of the elastic bars must permit the model to represent the in plane behavior of a thin plate subjected to normal and shearing stresses. The resisting in plane stresses and deformations must agree with the plane stress problem, the following conditions must be investigated:

1. When the model is subjected to uniform normal load of p per unit length in the x direction and up in the y direction deformations should correspond to those found by conventional methods of elastic analysis. The strains of the model in the x and y directions must be

$$\begin{aligned}\epsilon_x &= p(1-\nu^2)Et \\ \epsilon_y &= 0\end{aligned}\tag{A.1}$$

2. If the load p is applied in the y direction and up in the x direction the strains in the model are

$$\begin{aligned}\epsilon_x &= 0 \\ \epsilon_y &= p(1-\nu^2)Et\end{aligned}\tag{A.2}$$

3. For a uniform tangential load s per unit length, the shearing strain of the model must be

$$\gamma_{xy} = 2(1+\nu) s/Et \quad (A.3)$$

The discrete-element model representing the plane stress problem is shown in Figure 27 with joint loads which are the loads applied to the element in Figure 26. Taking section of a joint, equilibrium of the joint forces of the discrete-element model can be written as:

$$F_a + F_c = ph_y/2 \quad (A.4a)$$

and

$$F_b + F_c \sin \theta = ph_x/2 \quad (A.4b)$$

where

F_a, F_b, F_c = forces in bars a, b, and c, respectively;

θ = angle between bar a and bar c; and

h_x, h_y, h_2 = lengths of bars a, b, and c, respectively

The deformation of the model must correspond to the strain found by elastic analysis, as shown in Equation (A.1). Since the strain in the y direction is zero, the force in bar b must be zero. From Equation (A.4) the forces in bars a and c are:

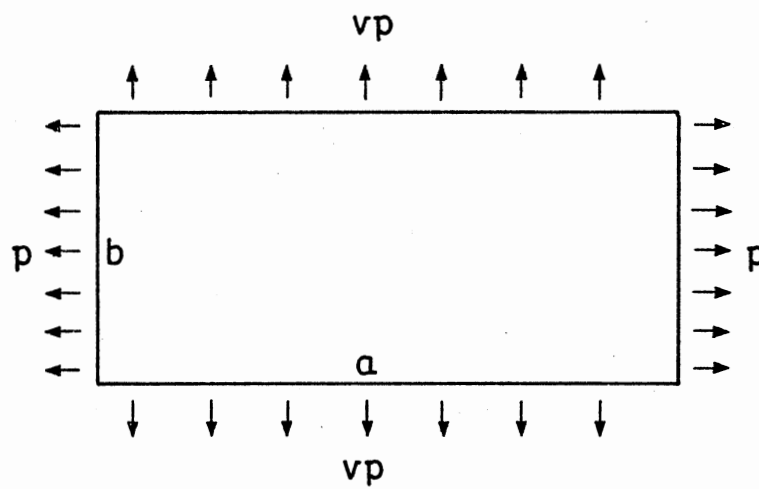
$$F_a = ph_y/2 - p(h_x)^2/2h_y \quad (A.5a)$$

$$F_c = ph_x h_2/2h_y \quad (A.5b)$$

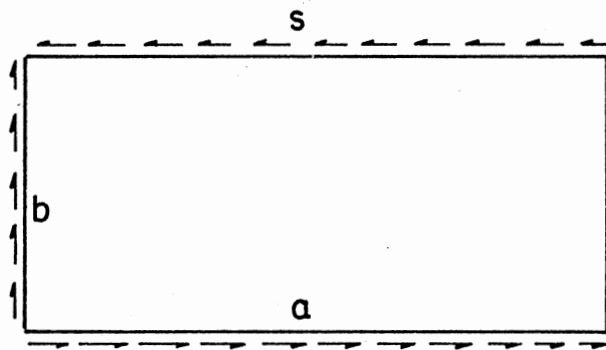
The strain in bar a is

$$\epsilon_a = F_a/E_a A_a = (ph_y/2 - p(h_x)^2/2h_y)/E_a A_a \quad (A.6)$$

where E_a, A_a are elastic modulus and cross section area of bar a. The strain of bar a must be the same as that given in Equation (A.1). By equating these two strains and rearranging, the cross-sectional area of bar a is found to be

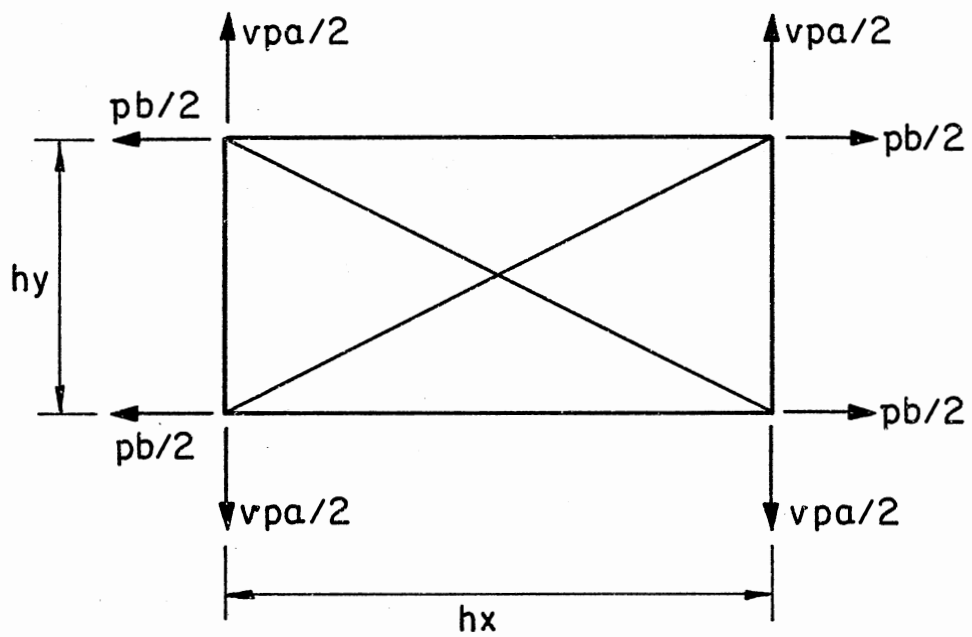


(a) NORMAL LOADING



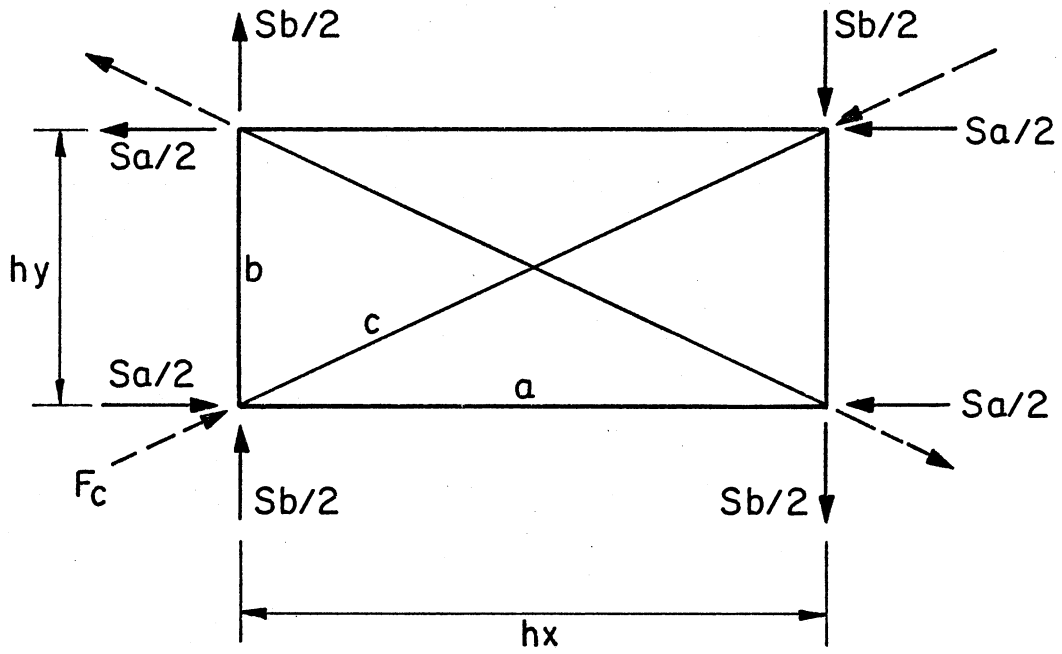
(b) PURE SHEAR

Figure 26. Plane Stress Element



(a) NORMAL LOADING

Figure 27. Member of Discrete-Element Model



(b) PURE SHEAR

Figure 27. (Continued)

$$A_a = \frac{+(h_y^2 - v h_x^2)}{2h_y(1-v^2)} \quad (A.7)$$

To determine the cross-sectional area of bar c, the deformations of bars a, b and c are related as follows:

$$h_y^2 = h_2^2 - h_x^2$$

Differentiating yields

$$h_y dh_y = h_2 dh_2 - h_x dh_x$$

Substituting $dh_x = \epsilon_a h_x$, $dh_y = \epsilon_b h_y$ and $dh_z = \epsilon_c h_z$

into the above equation yields

$$h_y^2 \epsilon_b = h_z^2 \epsilon_c - h_x^2 \epsilon_a$$

Since the strain in bar b is zero for the load condition under investigation, therefore

$$h_z^2 \epsilon_c = h_x^2 \epsilon_a$$

Replacing the strains by forces in the bars, bar areas and elastic constants, the area of bar c is related to the area of bar a by

$$A_c = h_2^2 F_c A_a E_a / h_x^2 F_a E_c \quad (A.8)$$

The forces F_a and F_c were evaluated in equation A.5 and letting E_a equal E_c , the area of bar c is found to be

$$A_c = \frac{vtH_2^3}{2h_x h_y (1-v^2)} \quad (A.9)$$

The cross-sectional area of bar b can be calculated by the same procedure. The loading described in the second condition will cause bars b and c to deform while the length of bar a remains unchanged.

The area of bar b is found to be

$$A_b = \frac{t(h_x^2 - v h_y^2)}{2h_x(1-v^2)} \quad (\text{A.10})$$

In the case when the tangential load s per unit length is applied to the plate element as shown in Figure 26 and equivalent joint forces applied to the model as shown in Figure 27, all horizontal and vertical bars of the model must be unloaded. This is necessary to insure zero normal strain in the horizontal and vertical directions. The forces in the diagonal bars are equal in magnitude but opposite in sense and are

$$F_c = (sh_x \cos \theta = sh_y \sin \theta)/2 \quad (\text{A.11})$$

The change in length of the diagonal bars, Figure 28, will be

$$\begin{aligned} \delta &= F_c h_z / A_c E_c \\ &= sh_z^2 / 2A_c E_c \end{aligned} \quad (\text{A.12})$$

The deformation of the element is shown in Figure 29 and the shearing strain is shown to be

$$\begin{aligned} 2 \tan (w) &= 2 \delta \sin \theta / h_x \\ &= sh_y h_z / h_x A_c E_c \end{aligned}$$

Equating the shearing strain in the model of theoretical shearing strain yields

$$\gamma_{xy} = sh_z h_y / h_x A_c E_c \quad (\text{A.13})$$

Equating equations A.3 and A.13, the area of bar c is found to be

$$A_c = \frac{h_z h_y t}{2h_x(1+v)} \quad (\text{A.14})$$

The area of bar c can satisfy both equations A.9 and A.14 only if

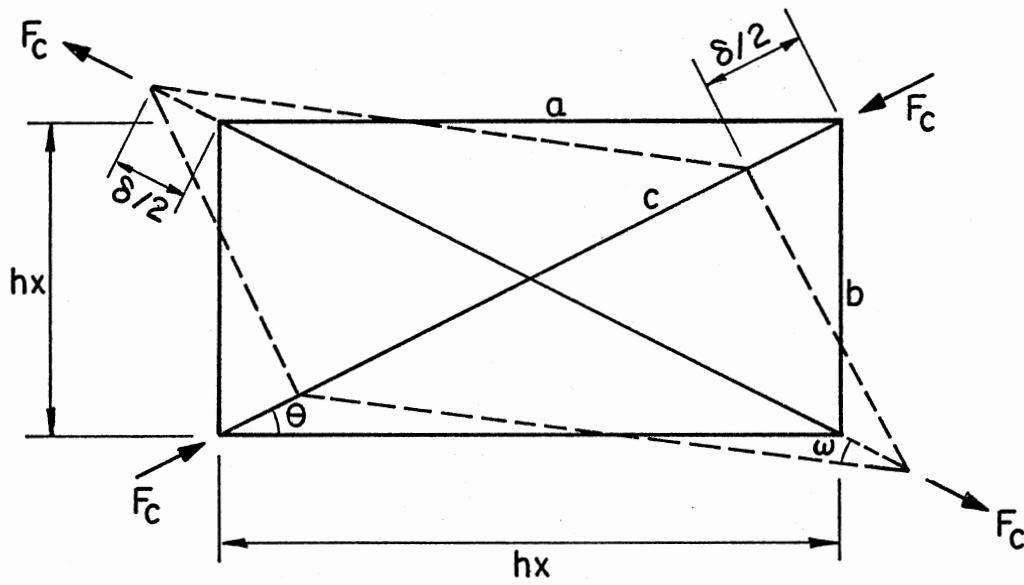


Figure 28. Shearing Deformation of Discrete Element

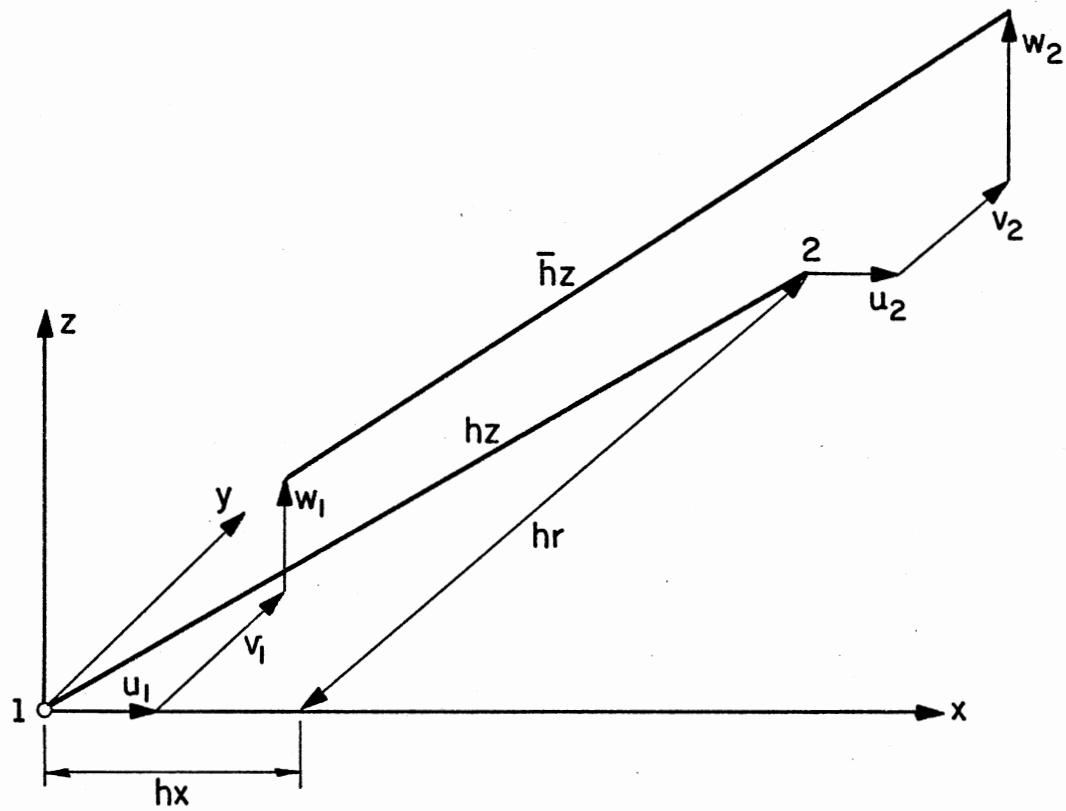


Figure 29. Deformation of an Elastic Bar of the Discrete Element

$$v = h_y/h_x^2 + h_z^2 \quad (\text{A.15})$$

Therefore, the Poisson's ratio depends on the geometry of the discrete element model given by Equation A.15. The Poisson's ratio will vary from 0.09 to 0.473 as the ratio for h_x/h_y varies from 3.0 to 0.333. However, it has been found (13) that the value of Poisson's ratio has little effect on the vertical displacement of the plate due to either vertical or inplane loads.

Force in an Elastic Bar

To calculate the forces in the elastic bar of a discrete element model, displacement, both vertical and in plane, are combined and include second order effects as described below. The original length of a bar in the x-y plane (Figure 30) is

$$h_z = (h_x^2 + h_y^2)^{1/2} \quad (\text{A.16})$$

Following joint displacements, the final length of the bar is

$$\bar{h}_z = [(h_x + \Delta u)^2 + (h_y + \Delta v)^2 + (\Delta w)^2] \quad (\text{A.17})$$

where \bar{h}_z = final length of the bar

$$\Delta u = u_2 - u_1$$

$$\Delta v = v_2 - v_1$$

$$\Delta w = w_2 - w_1$$

The axial strain of the bar can be written as

$$\epsilon = (\bar{h}_z - h_z)/h_z$$

or

$$\bar{h}_z = (h_z \epsilon + h_z) \quad (\text{A.18})$$

Equating equations A.17 and A.18 and rearranging terms gives

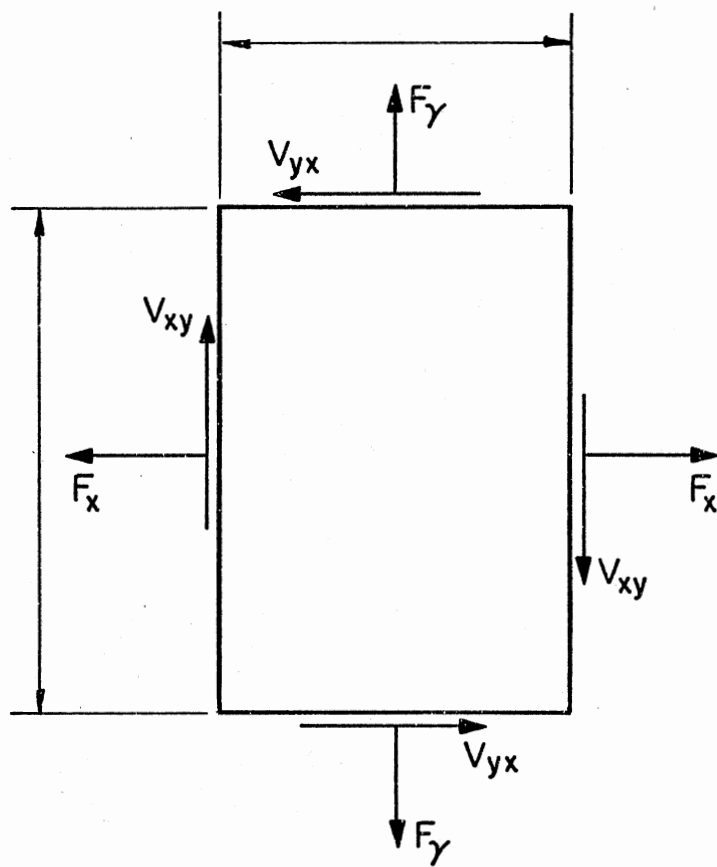


Figure 30. Plate Element With In-Plane Loads

$$\epsilon = \frac{h_x \Delta u + h_y \Delta v}{(h_z)^2} + \frac{(\Delta u)^2 + (\Delta v)^2 + (\Delta w)^2}{2(h_z)^2} \quad (\text{A.19})$$

$$\epsilon_x = (h_x + \Delta u) \epsilon / \bar{h}_z \quad (\text{A.20a})$$

$$\epsilon_y = (h_y + \Delta v) \epsilon / \bar{h}_z \quad (\text{A.20b})$$

$$\epsilon_z = \Delta w \epsilon / \bar{h}_z \quad (\text{A.20c})$$

Therefore the force of this bar in each principal direction is

$$P_x = EA \epsilon_x \quad (\text{A.21a})$$

$$P_y = EA \epsilon_y \quad (\text{A.21b})$$

$$P_z = EA \epsilon_z \quad (\text{A.21c})$$

The same procedure can be applied to bars that lie in the x and y directions. Equation A.21 is used to calculate the membrane forces.

Stresses from the Membrane

Model

To calculate the membrane stresses, consider a plate element in Figure A.5 subjected to inplane forces, the normal and shearing stresses are

$$\sigma_x = F_x / th_y \quad (\text{A.22a})$$

$$\sigma_y = F_y / th_x \quad (\text{A.22b})$$

$$\tau_{xy} = V_{xy} / th_y \quad (\text{A.22c})$$

$$\tau_{yx} = V_{yx} / th_x \quad (\text{A.22d})$$

A membrane element in Figure 31 is used to represent the plate element are applied directly to the joints of the model.

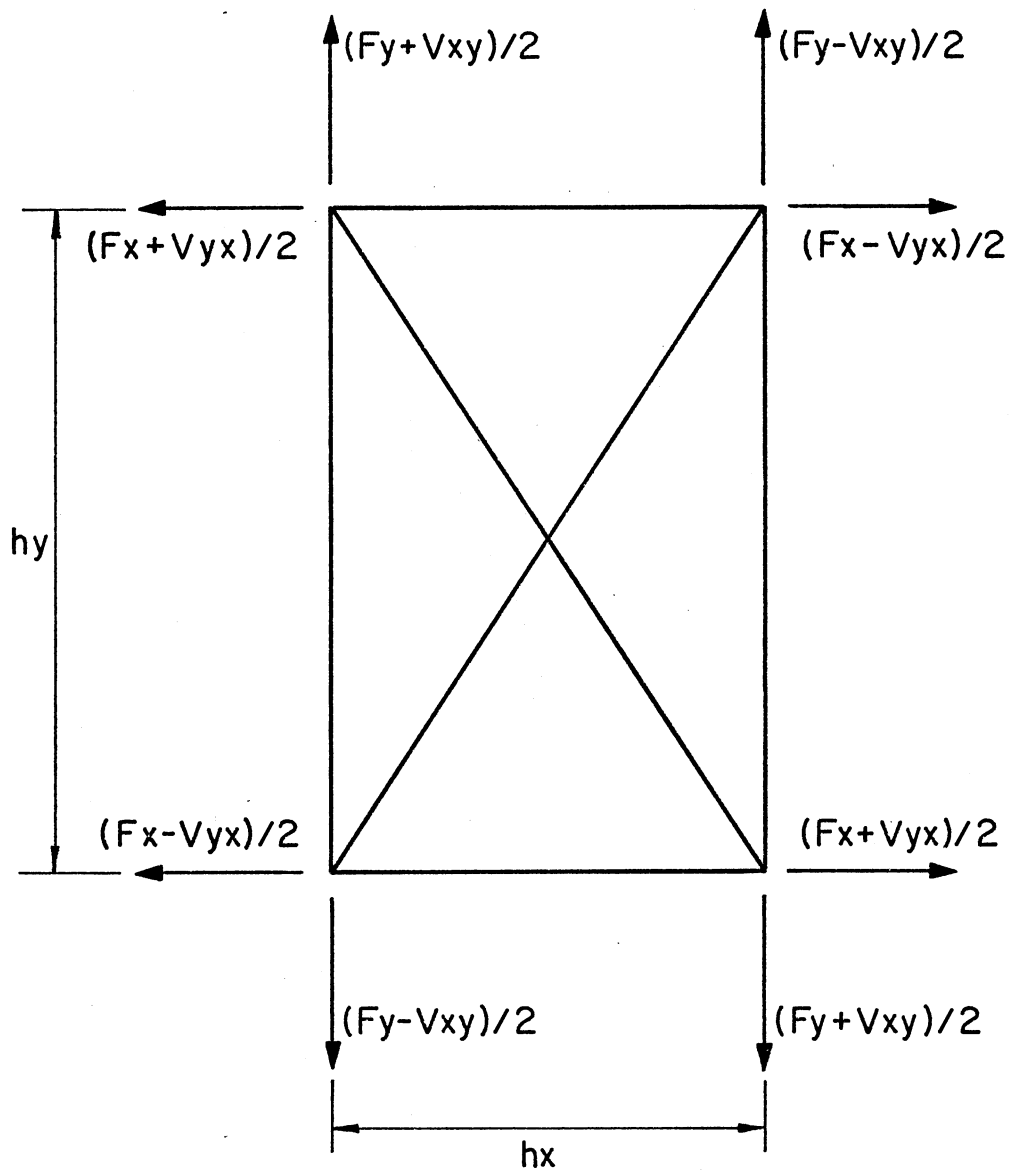


Figure 31. Discrete Element Representation of Plate Element

The axial force of each bar is calculated as described before and identified by the letters in Figure 32. The forces are calculated from the known joint displacements. The joint equilibrium equations for the model are

$$\begin{aligned}
 [F_B + F_H \cos \theta] &= [F_x + v_{yx}]/2 \\
 [F_C + F_H \sin \theta] &= [F_y + v_{xy}]/2 \\
 [F_B + F_E \cos \theta] &= [F_x - v_{yx}]/2 \\
 [F_D + F_E \sin \theta] &= [F_y - v_{xy}]/2 \\
 [F_A + F_E \cos \theta] &= [F_x - v_{yx}]/2 \\
 [F_C + F_E \sin \theta] &= [F_y - v_{xy}]/2 \\
 [F_A + F_H \cos \theta] &= [F_x + v_{yx}]/2 \\
 [F_D + F_H \sin \theta] &= [F_y + v_{xy}]/2
 \end{aligned} \tag{A.23}$$

Solving these equations yields

$$\begin{aligned}
 F_x &= [F_A + F_B] + [F_H + F_E] \cos \theta \\
 F_y &= [F_C + F_D] + [F_H + F_E] \sin \theta \\
 v_{xy} &= [F_H - F_E] \sin \theta \\
 v_{yx} &= [F_H - F_E] \cos \theta
 \end{aligned} \tag{A.24}$$

Substituting these values into equation A.22 gives

$$\begin{aligned}
 \sigma_x &= [F_A + F_B + (F_H + F_E) \cos \theta]/th_y \\
 \sigma_y &= [F_C + F_D + (F_H + F_E) \sin \theta]/th_x \\
 \tau_{xy} &= [F_H - F_E] \sin \theta/th_y \\
 \tau_{yx} &= [F_H - F_E] \cos \theta/th_x
 \end{aligned} \tag{A.25}$$

where F_A , F_B , F_C , F_E and F_H are shown in Figure 32.

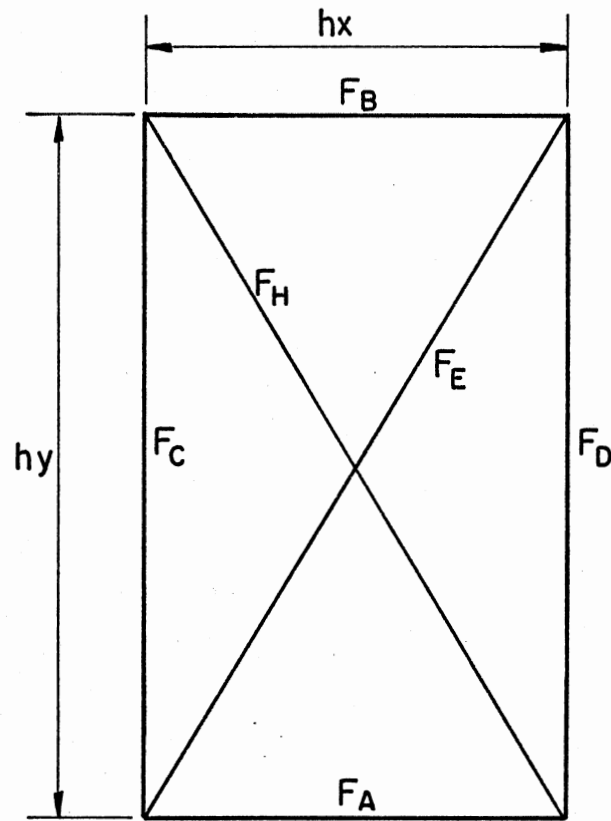


Figure 32. Forces in Elastic Bars of Membrane Element

APPENDIX B

DESIGN OF MINIMUM ANCHORAGE LENGTH

Consider the rheological model shown in Figure 33. This model has been formulated to represent the interaction of three physical quantities in the pullout test, the pullout force, the displacement and the strain of the reinforcement. In this model, this interaction is characterized by the length of reinforcement required to accommodate the input force. The results of the laboratory pullout tests were used to evaluate the resistance coefficient and displacement and strain of the fabric for a given pullout force. These parameters were then used in the solution to the soil-reinforcement interaction equation to predict the length of fabric required for a given pullout force. Comparisons between lengths of fabric measured and lengths of fabric predicted were excellent, considering the simple linear model utilized. Derivation of this simple soil-reinforcement interaction equation is as follows: As shown in Figure 33, one element of reinforcement is broken into p parts. Each part is acted upon by friction force, R_i ($i=1, p$), and is connected to its neighbor by a spring with a spring constant K . The external force F_p to the p part causes a displacement, u_0 , on the p part.

Considering the summation of forces on the n^{th} part it follows that

$$-K(u_{n+1} - 2u_n + u_{n-1}) = R_n$$

and hence

$$-K\Delta x \left[\frac{u_{n+1} - 2u_n + u_{n-1}}{\Delta x^2} \right] = \frac{R_n}{\Delta x}$$

taking limits

$$K \frac{d^2 u}{dx^2} + R = 0 \quad (\text{B.1})$$

The tensile force at each spring is dependent upon the friction force acting on the surface of each part of an element of reinforcement.

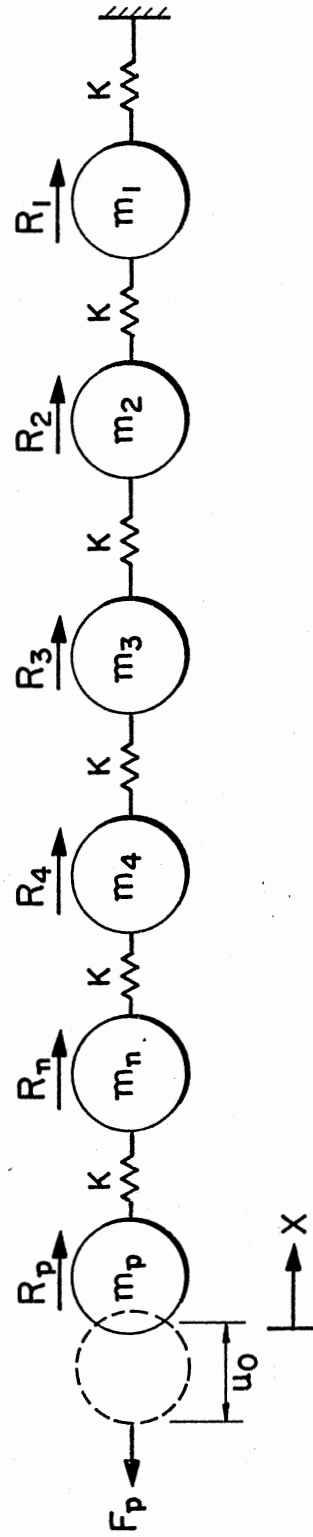


Figure 33. Rheological Model

The friction force, R , acting on each part is dependent on the displacement u of each part. From Equation B.1 it follows that:

$$K \frac{d^2 u}{dx^2} + R = 0 \quad \text{where } K = Fu \quad (\text{B.2})$$

The parameter, R represents the friction force which is dependent upon displacement. The parameter K which contains the externally applied force, F , represents how a tensile force in each spring is dependent on displacement and therefore varies along the length of an element of reinforcement.

The expression now becomes

$$Fu \frac{d^2 u}{dx^2} + R = 0 \quad (\text{B.3})$$

Solution of this equation is as follows: If R is dependent on displacement and is taken to be equal to some resistance coefficient, ρ_r , times the displacement, u , Equation B.3 becomes,

$$Fu \frac{d^2 u}{dx^2} + \rho_r u = 0 \quad (\text{B.4})$$

where ρ_r is defined as $\frac{Rn}{\Delta x}$.

Integrating Equation B.4 twice, it follows that

$$u = \frac{-\rho_r x^2}{2F} + C_1 x + C_2 \quad (\text{At } x=0 \quad u=u_0, \quad \frac{du}{dx} = u'_0)$$

$$u = -\frac{\rho_r x^2}{2F} + u'_0 x + u_0 \quad (\text{B.5})$$

Where ρ_r is a resistance coefficient which represents the friction force per unit length on the surface of the n^{th} part of an element of reinforcement; F is the external force applied to an element of reinforcement; x is the distance along the element of reinforcement from the point

of application of the applied force; u'_0 is the strain of a point at the application of an applied force and u_0 is the displacement of a point at the application of an applied force.

Design Considerations

To evaluate the length of reinforcement, L , the following procedure is suggested.

1. Evaluate the design pullout force F .
2. Perform a laboratory test on a reinforcement strip having the same material and geometric properties as the strip to be used in the field. The length of the strip can be equal to the length of the strip used in the pullout tests.
3. Using the pullout force F_L required to slide the test strip from the pullout test apparatus, the displacement u_0 , and the strain, u'_0 , of the reinforcement, evaluate the resistance coefficient ρ_r , using Equation B.5.
4. Design the strip for a displacement u_0 , and strain u'_0 , that is compatible with the pullout force F .
5. Evaluate the required length of reinforcement, L , by using the displacement, u_0 , the strain, u'_0 , and the resistance coefficient ρ_r , in Equation B.5, and
6. Apply a reasonable factor of safety to the length of reinforcement, L and/or accept an allowable probability of failure of the reinforcement.

APPENDIX C
EXAMPLE PROBLEMS

Example Problem No. 1

A column foundation is to be designed. The data and solution follow.

Data:

Column load = 50T

Soil configuration: deep sand deposit

Standard penetration test: $N = 15$

Foundation level: -2 ft

Tensile strength of fabric = 1000 lb/in.

Allowable maximum fabric deformation = 0.5 in.

Solution:

Try 4' x 4' footing.

$$a = 4', K = 10 \text{ T/ft}^3, \text{ depth ratio} = 0.5$$

Substituting into Equation (5.2) (see Figure 34):

$$A = 8.3'$$

Solving for t (Equation (5.3)):

$$T = 45 \text{ lb/in.}$$

Example Problem No. 2

Given a homogeneous embankment, the slope is 100 feet high, and rises at an angle of 35° with the horizontal. The properties of the soil are as follows:

$$s = 850 + \sigma \tan \phi \text{ psf}$$

$$\delta_m = 115 \text{ lb/cu ft}, \Delta_o = 12 \text{ in.}$$

$$\sigma_{\max} = 1000 \text{ lb/in.}$$

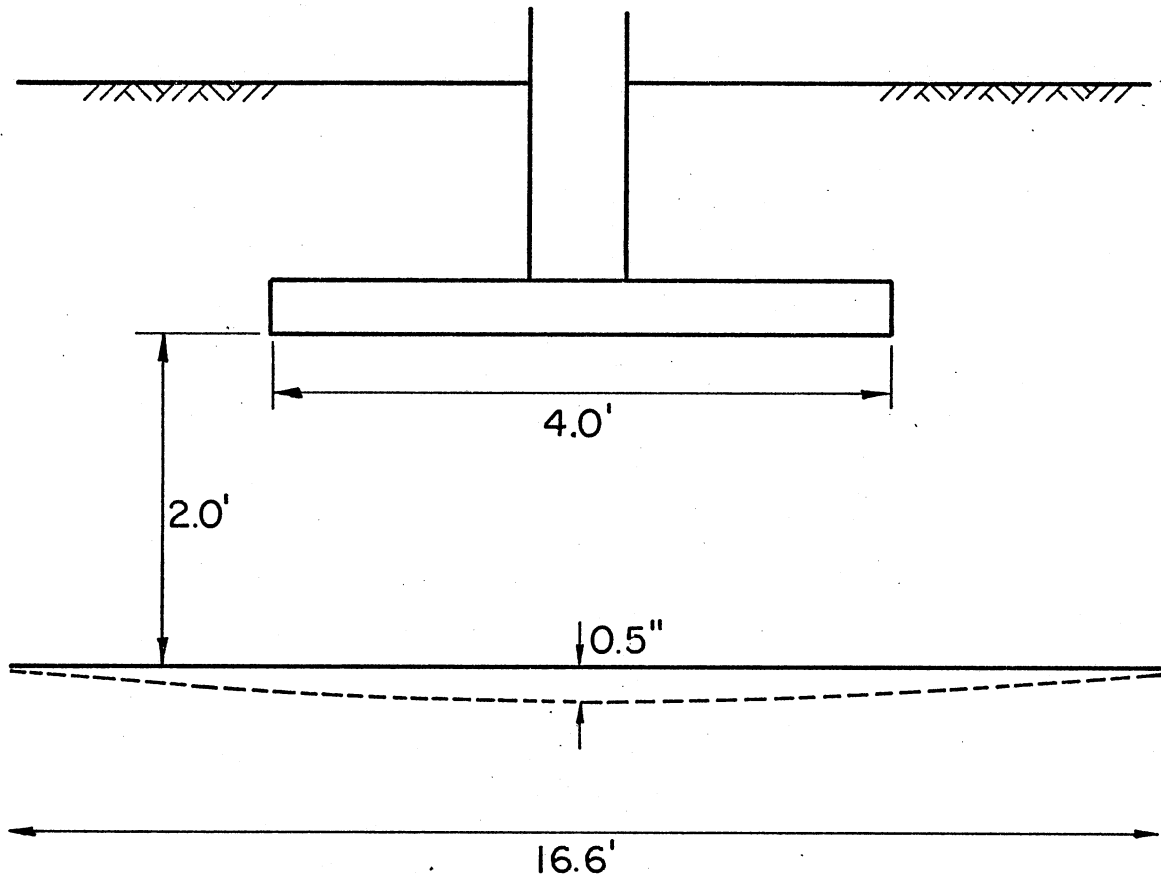


Figure 34. Deformed Fabric

Solution:

$$\begin{aligned} \text{Factor of safety} &= \frac{R\Sigma [C\Delta L + W\cos\alpha\tan\phi]}{R\Sigma W\sin\alpha} \\ &= \frac{319.3}{342.4} = 0.93 \text{ unsafe} \end{aligned}$$

Now to change the factor of safety to 1.00, the stabilizing moment should be equal to:

$$M = 1.00 \times 342.4R = 342.4R \text{ kip-ft}$$

But,

$$M = 319.3R + \Sigma T_i R$$

$$\Sigma T_i R = 23.1R \text{ kip-ft}$$

$$\therefore \Sigma T = 23.1 \text{ kip}$$

Assuming the pullout test was conducted and yields the following results:

$$r = 40 \times 10^{-3} \text{ kip/ft}$$

$$u_o = 0.55 \text{ in.}, u'_o = 0.05 \text{ in.}, T_L = 1.21 \text{ kip/ft}$$

$$\frac{\Delta_o}{2} = 6 \text{ in.}$$

$$T_F = \frac{1.21 \times 6}{0.55} = 11 \text{ kip} < 1000 \text{ lb} \times 12 = 12 \text{ kip/ft}$$

1. Using:

$$\delta = 6.0 \text{ in.}, u'_o = 0.05, T_F = 11 \text{ kip,}$$

and

$$p_r = 30 \times 10^{-3} \text{ kip/ft}$$

$$l_r = 41 \text{ ft (Equation (B.5))}$$

From Equation (5.7),

$$\delta = 5.50 \text{ in.}$$

2. Required:

$$\Delta M = 23.1 \times 10.0 = 3234 \text{ kip-ft}$$

$$\Delta M \text{ for one fabric} = 11 \times 135 = 1485 \text{ kip-ft.}$$

3. Use three fabrics as shown in Figure 35.

Example Problem No. 3

Solve Example Problem No. 3 using the following data. Cohesion and angle of internal friction gave the following results:

Test	C (psi)	ϕ
1	834	12
2	845	14
3	862	13
4	870	16
5	840	18

Fabric Tests	σ (lb/in.)
1	980
2	1100
3	1080

Solution:

C Analysis

Assume:

$$h(\theta) = \frac{1}{2\pi \times 1000} e^{-\frac{1}{2 \times 1000} (C - 880)^2}$$

From the sample we have:

$$\bar{C} = 850.2 \text{ psi}$$

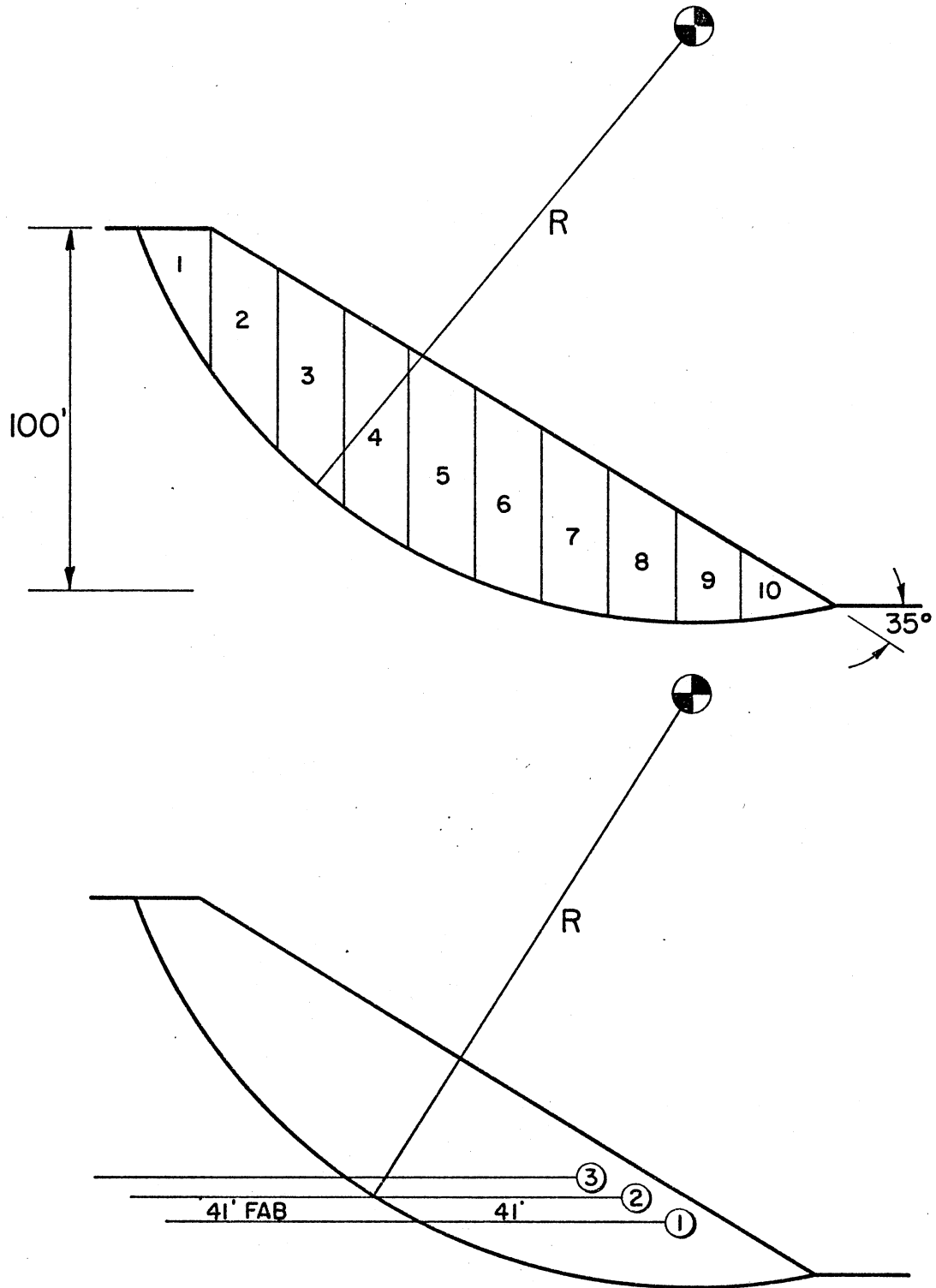


Figure 35. Reinforced Embankment

$$s^2 = \frac{\sum(C - \bar{C})^2}{n-1} = 231.2$$

$$E(\theta/y) = \frac{\frac{880}{1000} + \frac{5 \times 850.2}{231.2}}{\frac{1}{1000} + \frac{5}{231}} = 851.5 \text{ psi}$$

ϕ Analysis

Assume:

$$h(\theta) = \frac{1}{2\pi \times 240} e^{-\frac{1}{2 \times 240} (\phi - 11)^2}$$

From the sample we have:

$$\bar{\phi} = 14.6 \text{ in.}$$

$$s^2 = 5.8$$

$$E(\theta/y) = \frac{\frac{11}{240} + \frac{5 \times 14.6}{5.8}}{\frac{1}{240} + \frac{5}{5.8}} = 14.5 \text{ in.}$$

σ Analysis

Assume:

$$h(\theta) = \frac{1}{2\pi \times 100} e^{-\frac{1}{2 \times 100} (\sigma - 1000)^2}$$

From the sample we have:

$$\bar{\sigma} = 1053$$

$$s^2 = 5180$$

$$E(\theta/y) = \frac{\frac{1000}{100} + \frac{3 \times 1053}{5180}}{\frac{1}{100} + \frac{3}{5180}} = 1003 \text{ lb/in.}$$

Thus the expected values are:

$$C = 851.5 \text{ psi}$$

$$\phi = 14.5^\circ$$

$$\sigma = 1003 \text{ lb/in.}$$

VITA²

Aly Mahmoud Fawzy

Candidate for the Degree of

Doctor of Philosophy

Thesis: ELEMENTS OF FABRIC-REINFORCED SOIL BEHAVIOR

Major Field: Civil Engineering

Biographical:

Personal Data: Born in Cairo, Egypt, January 9, 1953, the son of Mr. and Mrs. Mahomoud Fawzy.

Education: Graduated from Cairo University, Cairo, Egypt, with the Bachelor of Civil Engineering degree in July, 1974; received the Master of Science degree in Civil Engineering from Oklahoma State University in July, 1977; completed requirements for the Doctor of Philosophy degree at Oklahoma State University in July, 1979.

Professional Experience: Teaching assistant, Cairo University, from July, 1974, to July, 1976; teaching assistant, Oklahoma State University, from September, 1976, to May, 1979.

Honor Societies: Member, Phi Kappa Phi and Chi Epsilon.